AD-A097 461 CALIFORNIA UNIV BERKELEY DEPT OF MECHANICAL ENGINEERING F/G 20/4
TURBULENT FLOW AND HEAT TRANSFER IN PASSAGE AROUND 180 DEGREE B--ETC(U)
FEB 81 J A HUMPHREY, B E LAUNDER N00014-80-C-0031

UNCLASSIFIED NL

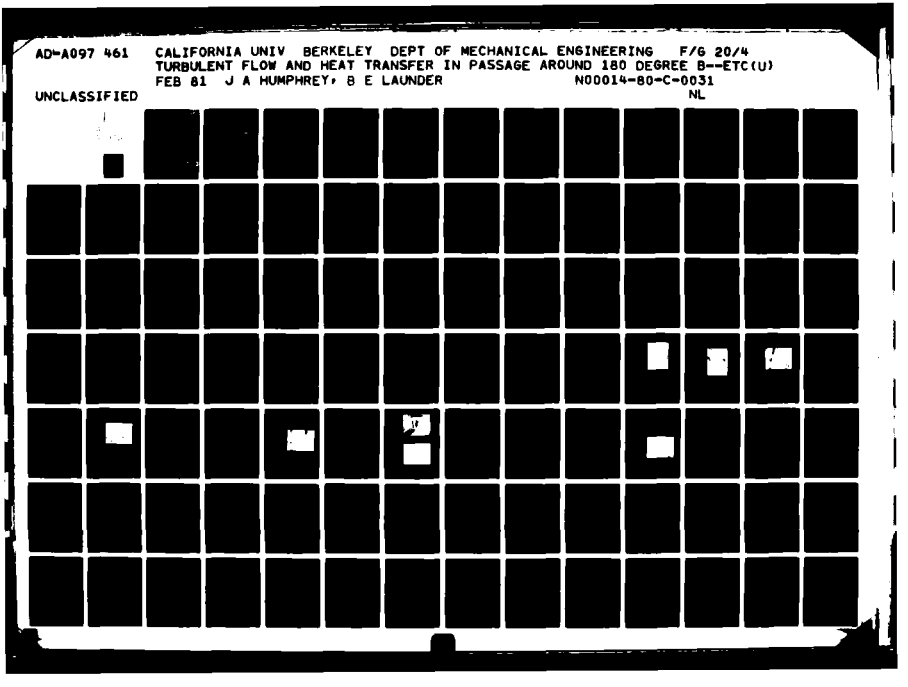

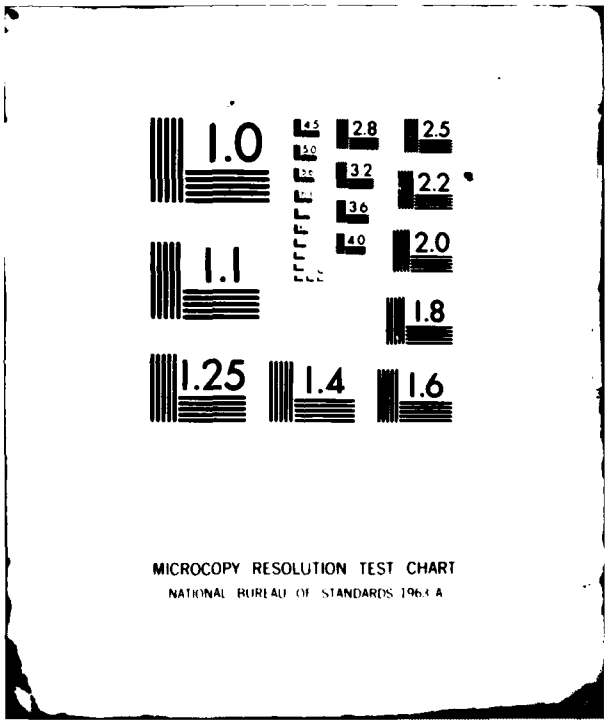
1.0
1.1
1.25
1.4
1.6
1.8
2.0
2.2
2.5
2.8
3.2
3.6
4.0
MICROCOPY RESOLUTION TEST CHART
NATIONAL BUREAU OF STANDARDS 1963 A

TURBULENT FLOW AND HEAT TRANSFER IN PASSAGE AROUND 180° BEND - AN EXPERIMENTAL AND NUMERICAL STUDY

Annual Technical Report

September 1980

by

Joseph A.C. Humphrey
Assistant Professor
Dept. of Mech. Eng.
University of California
Berkeley, CA. 94720
U.S.A.

and

Brian E. Launder
Professor and Head of the
Division of Thermodynamics
and Fluid Mechanics
Dept. of Mech. Eng.
University of Manchester
Institute of Science and
Technology
Manchester M60 1QD
ENGLAND

Prepared for
M.K. Ellingsworth, Program Monitor
The Office of Naval Research
Arlington, Virginia 22217

Under Contract No. N00014-80-C-0031, work unit NR 097-440

SECURITY CLASSIFICATION OF THIS PAGE (When Data Entered)

REPORT DOCUMENTATION PAGE

READ INSTRUCTIONS BEFORE COMPLETING FORM

1. REPORT NUMBER: N00014-80-C-0031A (dcg)
2. GOVT ACCESSION NO.: AD-A097 461
3. RECIPIENT'S CATALOG NUMBER:

4. TITLE (and Subtitle): Turbulent Flow and Heat Transfer in Passage Around 180° Bend-An Experimental and Numerical Study.
5. TYPE OF REPORT & PERIOD COVERED: Yearly (Summary) Oct.1,1979-Sept.30,1980
6. PERFORMING ORG. REPORT NUMBER:

7. AUTHOR(s): Joseph A.C. Humphrey and Brian E. Launder
8. CONTRACT OR GRANT NUMBER(s): N00014-80-C-0031

9. PERFORMING ORGANIZATION NAME AND ADDRESS: Department of Mechanical Engineering, University of California, Berkeley, Ca. 94720
10. PROGRAM ELEMENT, PROJECT, TASK AREA & WORK UNIT NUMBERS: 19 191

11. CONTROLLING OFFICE NAME AND ADDRESS: Office of Naval Research, 800 N. Quincy Street, Arlington, Va. 22217
12. REPORT DATE: Feb[illegible]81
13. NUMBER OF PAGES: 101

14. MONITORING AGENCY NAME & ADDRESS (if different from Controlling Office): Annual summary rep. Oct 1-30 Sept 80
15. SECURITY CLASS. (of this report): Unclassified
15a. DECLASSIFICATION/DOWNGRADING SCHEDULE:

16. DISTRIBUTION STATEMENT (of this Report): Approved for Public Release; Distribution Unlimited

Accession For
NTIS GRA&I [X]
DTIC TAB [ ]
Unannounced [ ]
Justification
By
Distribution/
Availability
Dist | Special
A

17. DISTRIBUTION STATEMENT (of the abstract entered in Block 20, if different from Report): Same as Block No. 16

18. SUPPLEMENTARY NOTES:

19. KEY WORDS (Continue on reverse side if necessary and identify by block number): Turbulence Modeling, Curved Duct Flow, Laser Doppler Velocimetry, Numerical Computation, Finite Differencing, Heat Transfer, Algebraic Stress Modeling, Numerical Diffusion.

20. ABSTRACT (Continue on reverse side if necessary and identify by block number):
A review is presented of the first year of research performed in an investigation aimed at developing a calculation scheme for predicting general three-dimensional flows in curved passages of circular and square cross-section. The experimental component deals with the implementation and validation of a laser-Doppler velocimeter and associated instrumentation. The numerical component deals with the development of a technique for reducing numerical diffusion in the calculation scheme. An update is provided of the current status of the research. A tentative schedule of work for years two and three is also given.

DD FORM 1 JAN 73 1473 EDITION OF 1 NOV 65 IS OBSOLETE
S/N 0102 LF 014 6601

400 426

SECURITY CLASSIFICATION OF THIS PAGE (When Data Entered)

FOREWARD

The investigation described in this First Yearly Report to the Office of Naval Research (ONR) is the outcome of a continuing collaborative effort between the respective principal investigators, Professor Joseph A.C. Humphrey at the University of California, Berkeley (UCB), and Professor Brian E. Launder at the University of Manchester Institute of Science and Technology (UMIST). Because the first six months of this work were conducted while Professor Launder was at the University of California, Davis, and because the first year of research has involved an especially close collaboration between the principal investigators in order to ensure continuing complementary research efforts at their respective institutions, it is appropriate that the first yearly report should be co-authored.

At UCB an experimental facility has been constructed which allows the measurement of fluid velocity and turbulence characteristics in and downstream of curved ducts of square or circular cross-section using an automatic data acquisition system. A corresponding heat-transfer experiment for flow in ducts of circular cross-section is in preparation at UMIST. A numerical procedure for predicting turbulent flow in and downstream of curved ducts of square cross-section is under development at UCB. A corresponding effort for predicting flows in ducts of circular cross-section is being developed at UMIST. It is important to note that while the two calculation schemes differ in their coordinate geometry (cylindrical versus toroidal) the numerical approach and, especially, the turbulence modeling, are the same. As work progresses, measurements, calculations and the numerical schemes under development at the two institutions will be critically compared and evaluated for the benefit of both.

In several important ways the first year of research for ONR has overlapped with a one year program of research conducted by Professor Humphrey at UCB for the National Science Foundation (NSF). Thus, while the ONR program has benefited from the experimental facility and preliminary numerical explorations initiated with NSF funds, the NSF program has benefited from continuing and extensive numerical developments made possible by ONR. We believe that this overlapping of programs, from which a mere duplication of research efforts has been strickly barred, has strongly benefited both investigations and the study of curved duct flows in general. We wish to express our appreciation to Dr. Win Aung of the National Science Foundation and Dr. Keith Ellingsworth of the Office of Naval Research for permitting and encouraging this mutually beneficial program interaction.

This report is, primarily, an account of the work performed for ONR throughout the first year (1979-1980) of research. However, because the work overlaps with the study performed for NSF during the same period of research, reference will be made to the latter and to an oncoming final NSF report. Upon completion, the NSF document will serve as an iterim ONR report and will be made available to those individuals on the ONR distribution list wishing to receive a copy.

ABSTRACT

An account is rendered of the research conducted during the first year of an investigation aimed at developing a computational facility for predicting turbulent flow in 180° curved passages of rectangular and circular cross-section. In order to evaluate critically the numerical scheme and turbulence model under development an experimental apparatus for measuring the velocity and turbulence characteristics of such flows has been constructed.

The first year of research has been dedicated primarily to:

1. Developing, testing and running the experimental apparatus and associated electronic instrumentation (including a computer-aided automatic data acquisition system).
2. Developing and testing a quadratic-upstream convective differencing scheme to alleviate the problems of numerical or "false" diffusion associated with simple upwind differencing.

Progress made on these two accounts is reviewed particularly in relation to the overall objectives of this research program. An evaluation is made of the present status of the program and a tentative schedule of projected activities is outlined for years two and three of research.

1. REMINDER OF THE PROBLEM OF INTEREST

It has only been relatively recently (the past 6-7 years) that numerical techniques and models of turbulence have been applied to the problem of predicting complex three-dimensional (3-D) flows with heat transfer. While there is a clear indication in the literature that some measure of success has been achieved [1-10] there remain serious uncertainties relating to:

a) The efficiency and accuracy of the various numerical prediction schemes.

b) The accuracy and generality of application of the various models of turbulence.

c) The rigurousness and generality of the tests applied to the numerical schemes and models of turbulence respectively.

Point (c) above is especially important since the rigorous testing of a turbulence model requires that *numerical* aspects of the problem be error free. Thus, for example, it would be desirable to reduce to a minimum numerical or "false" diffusion in a numerical procedure prone to this effect *prior* to establishing the relative merits (or demerits) of a particular model of turbulence.

The present work addresses each of the above three points by reference to 3-D turbulent flows within, and downstream of, 180° curved passages of circular and square cross-section. The choice of flow was dictated by two major considerations:

1. That is arise in the components of major industrial processes, such as, for example, bends in heat exchangers, and hence be of practical importance.

2. That is permit a rigorous and fairly general test of models of turbulence purporting to predict complex 3-D flows.

The flow entering a curved passage experiences a radial pressure gradient-centrifugal force imbalance which subjects slow-moving fluid near the side walls (parallel to the plane of curvature) to a pressure force which drives the flow from the outer radius wall towards the inner radius wall. Continuity demands that a corresponding flow be set up along the curved passage symmetry plane from the inner to outer-radius wall. This motion is referred to as secondary motion of the "first" kind. In the straight section following the curved passage the secondary motion relaxes through turbulence diffusion and redistribution processes. If the straight duct is long enough this cross-stream flow is replaced by a weaker turbulent stress-driven secondary motion of the "second" kind.

The transition between the two states of cross-stream motion can only be predicted by a turbulence model in which Reynolds stresses are calculated from their respective transport equations. In addition, the model must be able to account for outer-wall destabilizing effects and inner-wall stabilizing effects on the flow in the curved section. It is clear that the combination of a curved duct followed by a straight section represents a severe and very general test case for *any* numerical model of turbulence.

2. RESTATEMENT OF RESEARCH PROGRAM OBJECTIVES

The research objectives of this investigation are two:

1. To develop, test and apply a numerical calculation procedure capable of modeling fairly general and complex 3-D flows, strongly affected by turbulence diffusion and redistribution processes.
2. To obtain the necessary experimental information by reference to which a precise and fairly extensive evaluation of the numerical model may be carried out.

With respect to the first objective, attention has been focused on the development of a so-called "semi-elliptic" type of calculation scheme. The scheme is of the global iteration class [11] wherein pressure is the only primitive variable stored three-dimensionally. A forward marching algorithm is used as part of a global iteration process in which streamwise diffusion contributions to the balance equations are neglected. Although, due to the nature of the forward-marching approach, imbalances (in continuity or in the representation of pressure gradients) are introduced in the system of governing equations, the iterative nature of the procedure allows their reduction by systematic correction until they are reduced to a negligible level.

The present scheme is based on a 3-D elliptic numerical procedure developed by Humphrey [8,12] but is being modified here to include the semi-elliptic method of Pratap [13] and the QUICK scheme for convective differencing of Leonard [14].

The second objective has been dictated by the general unavailability of sufficiently extensive and accurate experimental data concerning the turbulence characteristics of complex 3-D flows. The laser-Doppler velocimeter data measured by Humphrey [12] (see also reference [15]) alleviates the situation somewhat in that is provides a test for the numerical prediction of turbulent flow development in 90° curved ducts. However, to our knowledge there is no equivalent body of information for a 180° curved passage connected to a straight downstream section, in which the pressure dominated flow leaving the bend section relaxes through vigorous turbulent interactions. An experimental apparatus meeting the needs for obtaining such information with the help of a PDP 11/34 mini-computer is described in an Appendix attached to this report.

3. SUMMARY OF ACCOMPLISHMENTS FOR YEAR ONE

During the first year research efforts have been concentrated on:

1. Building and testing the experimental facility for measuring developing turbulent flows in ducts of circular and square cross-section.
2. Developing and testing a quadratic-upstream interpolation scheme for the finite differencing of convection terms in the Navier-Stokes equations.

The experimental facility is described in detail in the Appendix. Since its completion, however, it has been modified in several respects. The most significant changes have consisted in:

1. Replacing 4 out of 5 perforated plastic plates in the upstream duct by 3 metal screens of graduated mesh sizes.
2. Removing the globe valve in the upstream duct.
3. Removing the venturi meter from the downstream duct location and placing it on the pump line feeding the constant head tank.

In combination, these modifications have led to a much more uniform flow, of reproducible turbulence characteristics, in the straight section proceeding the 180° curved section.

The experimental system has been tested carefully and extensively. At the time of writing measurements are being completed for two velocity components and three Reynolds stresses at various stations in a 180° curved duct and downstream tangent of square cross-section. These are briefly discussed in Section 4.1 of this report. A considerably more detailed account of this work is forthcoming and will be submitted as part of a final report to NSF and an interim (1981-1982) report to ONR.

The quadratic upstream interpolation scheme is also described in detail in an appendix. The desirability of a convective-differencing

scheme free of false-diffusion error is obvious. The QUICK scheme has the advantage of possessing simultaneously the accuracy characteristic of central differencing and the stability characteristic of upwind differencing. As shown in the appendix QUICK can be made to work efficiently in the laminar flow regime and (with more difficulty) in the turbulent flow regime. The higher accuracy per grid node yielded by the QUICK approach (relative to the standard HYBRID practice embodied in the TEACH family of codes)* means that, in principle, calculations of a given accuracy can be made at a lower cost. This is a particularly important consideration for complex 3-D flows (such as the ones of interest here) requiring substantial grid refinement for their spacial resolution. While development and testing of the QUICK scheme has been performed in 2-D flow configurations, the scheme is presently being adapted and tested for the case of 3-D curved duct flow.

*From which the present numerical procedure ultimately derives, [16].

4. PRESENT STATUS OF THE RESEARCH PROGRAM

At the time of writing, the experimental, numerical and turbulence modeling aspects of this work continue to be developed. This section is intended to serve as a brief update of present activities at the Berkeley campus.

4.1 Experimental Measurements

Measurements are being concluded for turbulent flow conditions (Re ≈ 40,000) in a 180° curved duct of square cross-section* corresponding to the dimensions given in the Appendix. Two components of mean velocity (U_θ and U_r) and three Reynolds stresses ($\overline{u_\theta^2}$, $\overline{u_r^2}$ and $\overline{u_\theta u_r}$) are being determined in detail at longitudinal stations corresponding to $-5D_H$, 0°, 45°, 90°, 135°, 180°, $5D_H$, $10D_H$ and $20D_H$. Because of the amount of work involved, only the most critical longitudinal stations will include radial component measurements.

Samples of center-plane longitudinal velocity and turbulence intensity measurements are given in Figs. 1-a and b, respectively. The data for θ = 45° was not available at the time of plotting. The plots are provided here solely for qualitative discussion of the flow. A report to be submitted jointly to NSF and ONR will contain a detailed description of the flow in the curved passage and, of special significance to the ONR program, in the straight downstream duct.

---

*This geometry was originally proposed to NSF for investigation. The complex details of the flow relaxing in the straight section downstream of the bend, and the relative ease and accuracy with which data can be obtained through flat walls have made of this geometry a critical experimental case for the ONR research program on turbulence model development.

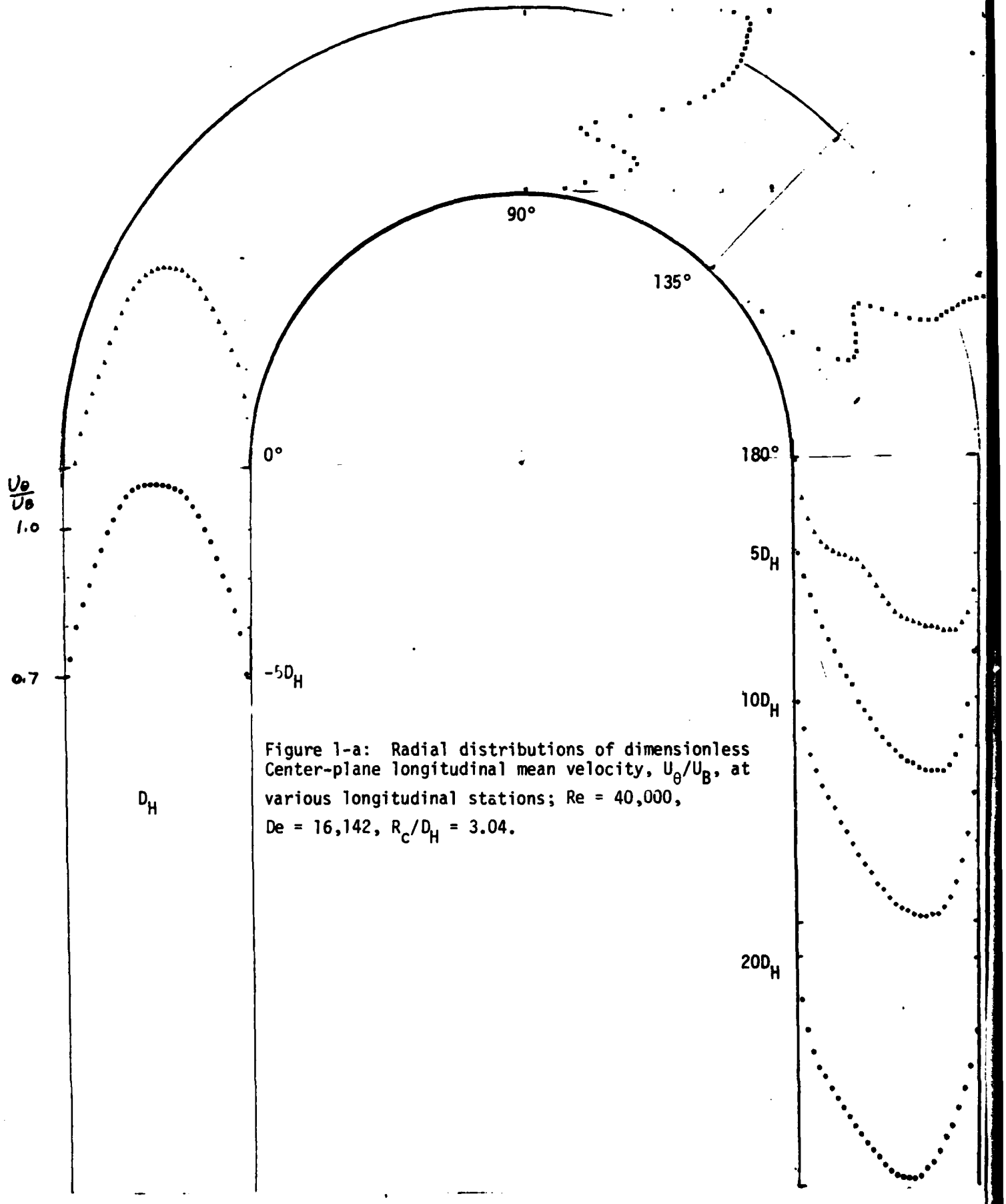

Figure 1-a: Radial distributions of dimensionless Center-plane longitudinal mean velocity, U_θ/U_B, at various longitudinal stations; Re = 40,000, De = 16,142, R_c/D_H = 3.04.

The peak velocity of the flow at $-5D_H$ in Fig. 1-a corresponds to 1.50 m/s. At this position the flow does not appear to be affected by the bend. At 0° the center plane profile has accelerated near the inner-radius wall, as would be expected from simple potential flow considerations. At 90° and 135° the main flow profiles show double peaks suggesting an intense secondary motion in the cross stream plane. At these locations the dampening influence (on the secondary motion) of the downstream straight duct is not yet felt. From 180° to $20D_H$ the flow commences a relaxation process which is incomplete at the $20D_H$ downstream station.

Corresponding turbulence intensity plots shown in Fig. 1-b point to various interesting aspects of this flow. Like the mean flow, at $-5D_H$ longitudinal turbulence characteristics are essentially fully developed. At this station the wall values of turbulence intensity are approximately 12%. At 90° and 135° secondary motions and shearing effects (particularly at the outer radius wall) produce triple peaks in the turbulence intensity radial distribution. The implication is that at these locations the flow is very mixed and anisotropic in its characteristics. Corresponding evidence of similar turbulence activity was not observed in the earlier 90° bend turbulent flow study of Humphrey, et al. [15]. It would seem that the presence of the downstream tangent as of 90° in [15] had an earlier stabilizing influence on the flow in the bend which, in the present results, appears as of 135° approximately. Similarly to the mean flow, the longitudinal intensity profiles show that the relaxation process taking place in the downstream duct is far from having been completed by $20D_H$.

These and similar detailed measurements at other transverse locations (offset from the center plane) will provide a critical base case for testing the numerical method and turbulence model under development.

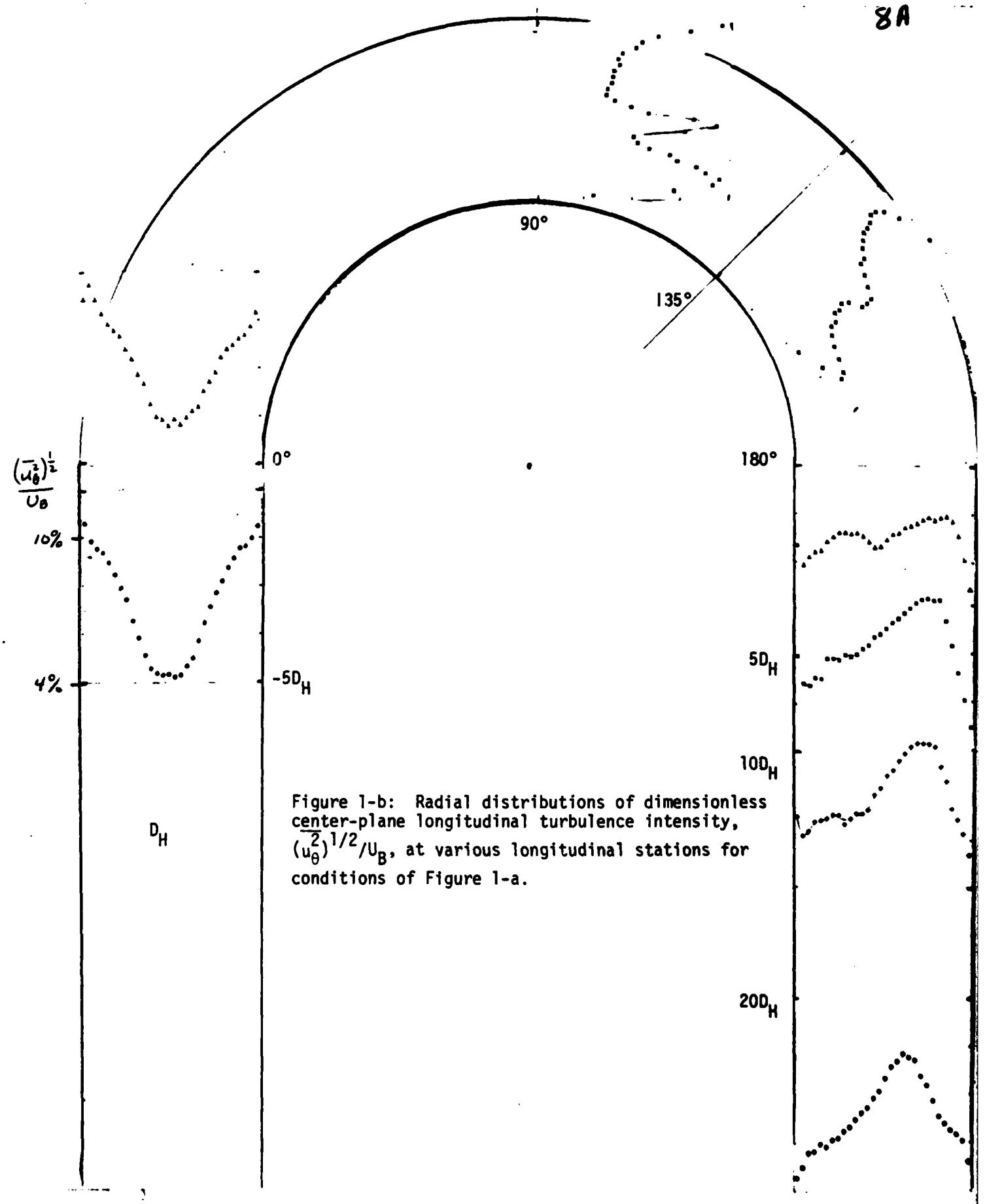

Figure 1-b: Radial distributions of dimensionless center-plane longitudinal turbulence intensity, $(\overline{u_\theta^2})^{1/2}/U_B$, at various longitudinal stations for conditions of Figure 1-a.

4.2 Turbulence Modeling

The details of the flows of interest to this study are strongly influenced by turbulent transport processes driven in part, by large anisotropic effects. Examples are the secondary flows arising in corners driven by gradients of turbulent stresses. These can only be predicted with a closure scheme solving for Reynolds stresses directly. The effective viscosity concept, based on the notion of a single velocity scale and length scale, has been shown [15] to yield qualitatively correct predictions of the principle average features of curved duct flow. However, it remains to be explored further.

A full Reynolds stress closure requires the solution of seven transport equations for turbulence quantities in a 3-D flow. While obtaining solutions to such equations is within current computational capabilities, there is a need for continued experimentation and computer optimization to determine the empirical constants arising in these more complex models. The simpler approach, based on the k/ε model of turbulence requires less computer time and core and may yield average flow results of comparable accuracy to the higher closure. The calculations of [15] were performed on a coarse grid* and it is not certain at this time what refinements, if any, would improve the use of the k/ε model for predicting the mean features of curved duct flows. Both closures will be of interest to this work, although emphasis will be placed on the Reynolds stress scheme.

---

*These were fully elliptic calculations and, by necessity, the grid was limited to 14 x 11 x 19 nodes. Numerical imprecisions arising from the coarse grid are, therefore, confounded with model limitations. The semi-elliptic calculation approach discussed in section 4.3 should allow a separation of the two effects.

In the two equation model [17], kinetic energy (k) and its dissipation (ε) are determined from respective transport equations. The rather simplistic turbulent viscosity concept does not possess the required breadth of applicability to be of universal value. However, turbulence models of this kind are still thriving and achieving surprisingly good results. One of the reasons for this success is well brought out by Bradshaw [18]. In many flows the turbulent shear stresses are at least two orders of magnitude smaller than typical dynamic pressure levels. Therefore, the turbulent shear gradients are most significant in thin localized shear layers. In flow regions where stress gradients are not large, gradients of static pressure provide the main force on the fluid elements. Because turbulence activities are partly suppressed by the cross-stream flow at the walls in a curved duct, radial pressure gradients dominate flow behavior. This point and economy of calculation are two strong justifications for pursuing a two-equation turbulence model approach.

The vertical flow emerging from a curved duct will commence a relaxation process in the straight downstream section. Every component of the Reynolds stress tensor plays an important role in the relaxation dynamics. A 3-D algebraic Reynolds stress model is presently being developed along the lines of Launder [19], and Rodi [20] to model this complicated flow.

The essence of the algebraic stress model lies in the recognition that through various simplifications the full Reynolds stress equations may be reduced to a set of algebraic relations among the Reynolds stresses, of the general form:

$$\overline{u_i u_j} = \overline{u_i u_j}\left(\overline{u_p u_q}\ ,\ \frac{\partial U_e}{\partial x_m}\ ,\ \varepsilon, k\right) \qquad (1)$$

Approaches of this kind have been used by Launder and Ying [21] and Tatchell [22] to predict turbulence driven secondary flows in ducts of square cross-section. Equations of the form (1) are obtained if stress gradients in the Reynolds stress equations are eliminated. The convective and diffusive transport of Reynolds stresses are related to the transport of turbulent kinetic energy by assuming that the rate of variation of $\frac{\overline{u_i u_j}}{k}$ along a streamline is much less than that of $\overline{u_i u_j}$ itself. A more general model of this type, in principle, should yield better predictions of considerably more complex turbulent flows than the standard k-ε model.

Presently, the algebraic stress model is being tested by reference to developing turbulent flow in ducts of rectangular cross-section [23]. Subsequently, predictions of 180° curved duct flow and of the flow emerging from a 180° curved duct and relaxing in a straight duct section will be compared with detailed measurements from this study (see section 4.1) and two equation (k/ε) model predictions. It is anticipated that the curved and relaxing flow tests will be especially useful in helping to determine the algebraic stress model accuracy and range of application. It is also anticipated that the curved-straight section flow comparison will yield some insight into the manner by which the algebraic approach can be made more accurate for modeling complicated 3-D anisotropic turbulent flows.

4.3 Numerical Procedure

Earlier k/ε model calculations of developing curved duct flows with strong curvature effects [15] yielded qualitatively acceptable results but did not clarify which of two effects, the turbulence model or numerical diffusion, was the most serious limitation in the calculations. The development of an algebraic stress model of turbulence (section 4.2) addresses the issue of resolving turbulence model failures. Improvements of a strictly *numerical* nature are discussed here.

In his doctoral thesis, Pratap [13] developed a semi-elliptic calculation approach which was applied to flows in curved ducts of relatively mild curvature [6]. The nature of the scheme is such that the pressure field is stored three-dimensionally and hence is dealt with in a fully elliptic manner. However, velocity components are stored in two-dimensional arrays which, together with the pressure field, are repeatedly iterated upon until the entire flow field satisfies a pre-established convergence criterion. A forward marching (parabolic-type) algorithm is used in the iteration process and requires that streamwise diffusion contributions to the balances of momentum be neglected. Likewise, regions of streamwise flow reversal are not allowed.

Notwithstanding these limitations, the semi-elliptic scheme is considerably more versatile than a purely parabolic calculation approach and allows for economy of calculation even on fairly refined grids. It has the virtue of *not* requiring special and (generally) complicated approaches for the calculation of pressure, such as those which are described in [11,24,25].

The present study is concerned mainly with developing flows of strong to mild curvature; $2 \leq R_C/D_H \leq 20$ approximately. Parabolic schemes for such flows have been shown to lead to inaccurate results [26] and improvements for predicting pressure as outlined in [11,24,25] have only been tested for fully developed flow conditions or for conditions where the flow entering the curved section comes directly from a contraction; the latter is a case of relatively thin boundary layer regions and, consequently, localized weak secondary flows. Fully elliptic calculations [7, 15, 26] are expensive and, due to storage limitations, cannot usually be performed with the degree of grid refinement necessary for producing grid-independent (numerical-diffusion uncontaminated) results.

Given the above, the semi-elliptic calculation approach presents the level of compromise required for this work if regions of possible flow reversal can be dealt with appropriately. Small regions with flow reversal have been observed experimentally (and computed) in the laminar flow regime by Humphrey, et al. [7]. Measurements available in the turbulent flow regime do not confirm, nor do they rule out, the possible existence of flow reversal, particularly at the inner-radius wall of a curved duct. One of the missions of the experimental study is to investigate possible flow separation and reversal between 90° and 180° streamwise locations.

Calculation instabilities produced by the (sometimes temporary) appearance of negative streamwise velocities in a semi-elliptic scheme can be overcome by following the suggestion of Bergeles [27] that, upon calculation, negative velocities and mass imbalance terms in the pressure correction equation be reset to zero. Implicit is the assumption that for calculation cells within the reversed flow region local continuity is satisfied. While this practice introduces an overall inaccuracy in the predicted results, the error is generally negligible relative to the considerably more refined, and hence more precise, calculations that the semi-elliptic approach allows. Of course, in those cases where flow reversal is only a temporary numerical nuisance, the practice allows the calculation scheme to converge to the correct final results without undesirable numerical instability creeping into the calculations.

4.4 Summary

Laminar and turbulent (k/ε) calculations using a semi-elliptic procedure similar to that described in [13] have already been performed for the 90° bend flow investigations of [7] and [15]. Prior to conducting these calculations the numerical scheme was carefully checked by reference to the

FIGURE 2: LAMINAR FLOW CALCULATIONS OF REFERENCE 30.

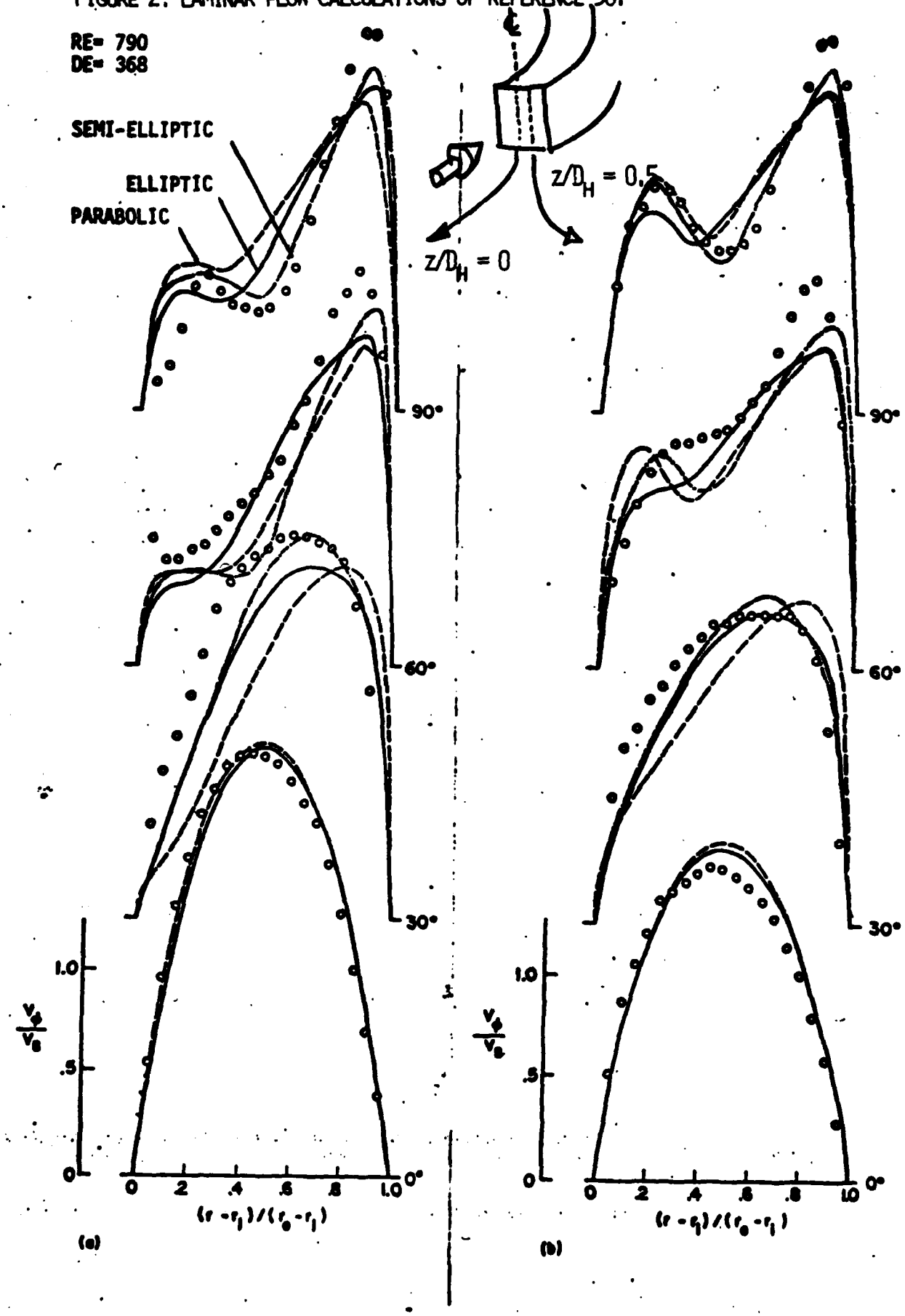

computation of developing laminar flow in a straight duct of square cross-section with and without one side wall sliding transverse to the main flow direction. Excellent agreement was found between the calculations and the test case data. Figure 2 shows a sample of the results achieved for the 90° bend laminar flow case of [7]. Contrasted with the semi-elliptic results are calculations for the same flow using parabolic and fully-elliptic schemes. It is seen that, although imperfect, the semi-elliptic calculations most closely approximate the measurements. Improved agreement was subsequently obtained (using the semi-elliptic scheme) by modifying the exit plane boundary condition treatment. Although not shown here, the improved semi-elliptic calculation results predict very accurately the peaks and valleys in the laminar flow experimental data. It is anticipated that implementation of the higher order QUICK scheme for convective differencing will further enhance the accuracy of the semi-elliptic calculation approach for curved duct flows.

Presently, calculations using the algebraic stress model are underway for the 90° bend turbulent flow of [15] and the 180° experimental study discussed in section 4.1. In addition, k/ε model predictions of the 180° flow will be conducted for comparison with measurements and algebraic stress results.

In total, the 90° bend calculations are the subject for a communication to be presented at the AFOSR-HTTM-STANFORD Conference on Complex Turbulent Flows: Comparison of Computation and Experiment. The purpose of this conference is to evaluate numerical and turbulence modeling schemes.

Both the 90° bend flow calculations and the 180° bend-straight section measurements and calculations alluded to in this report will be the subject of a final report to be submitted jointly to NSF and ONR in May 1981.

5. PROJECTED RESEARCH SCHEDULE FOR YEARS TWO AND THREE

This section provides a tentative research schedule (in the form of a table) for work to be conducted at Berkeley during years two and three of research. The schedule reflects the need to operate on a flexible basis with a related program of research under the direction of Professor B.E. Launder at the University of Manchester Institute of Science and Technology (UMIST).

TABLE 1 : TENTATIVE RESEARCH SCHEDULE FOR YEARS TWO AND THREE

RESEARCH TOPIC	DEADLINE	COMMENTS
Completion of laser-Doppler velocimeter measurements of mean velocity and turbulence characteristics in and downstream of a 180° curved duct of square cross-section (strong curvature).	May 15, 1981	These results will provide the necessary basis for testing the accuracy and range of application of the algebraic stress model in combination with the semi-elliptic calculation scheme.
Completion of algebraic stress and k/ϵ model calculations of 90° and 180° turbulent flows in and downstream of strongly curved ducts of square cross-section. Comparison with experimental data. Inclusion of QUICK scheme in curved flow calculations and evaluation of advantages and disadvantages associated with QUICK.	July 15, 1981	The 90° results will be presented at the 1981 Stanford Shear Flows Conference. Both the 90° and 180° results will be written up as a joint report to NSF and ONR.
Completion of laser-Doppler velocimeter measurements of mean velocity and turbulence characteristics in and downstream of a 180° curved duct of circular cross-section (mild curvature).	September 30, 1981	The semi-elliptic toroidal coordinate calculation scheme will be developed at UMIST under the direction of Professor B.E. Launder. It will be based on the existing fully elliptic scheme described in [8] and, basically, will include the same algebraic stress model of turbulence of this work.
Inclusion of heat transfer in the respective UCB and UMIST calculation schemes. Continued curved pipe flow measurements of mean velocity and turbulence characteristics at UCB. Heat transfer experiments at UMIST.	September 30, 1982	The square cross-section geometry will be dealt with in UCB, while the circular cross-section will be dealt with at UMIST. The detailed breakdown of activities planned for the 1981-1982 period is not yet known at this time.

ACKNOWLEDGEMENTS

At various stages different individuals have directly or indirectly contributed to this continuing study on curved duct and pipe flow. Thanks are due to S. Li, N. Al-Shama and G. Beshouri who, through successive masters theses designed and built the flow system. This was done with the most valuable assistance from G. Lewis, L. Grout and W. Gandola of the Mechanical Engineering Machine Shops. A. Modavi was responsible for implementing the computerized data acquisition system and, together with J. Sabnis, was invaluable in helping to acquire the main body of experimental data alluded to in this report. S.M. Chang and T. Han have been responsible for developing the numerical aspects of the investigation. S.M. Chang was primarily involved with adapting an existing elliptic scheme to a semi-elliptic approach while T. Han was mostly concerned with developing the higher order QUICK convective differencing method and the algebraic stress model of turbulence. Thanks are due to M. Sindir for his generous cooperation and help in making quick progress with the algebraic stress model.

REFERENCES

1. Bergeles, G., Gosman, A.D. and Launder, B.E., "The Turbulent Jet in a Cross Stream at Low Injection Rates: A Three-Dimensional Numerical Treatment," Numerical Heat Transfer, Vol. 1, 217 (1978).

2. Bergeles, G., Gosman, A.D. and Launder, B.E., "Double-Row Discrete-Hole Cooling: AN Experimental and Numerical Study," ASME Winter Annual Meeting, San Francisco, 1978, Volume on Heat Transfer in Turbine - Hot Sections Components.

3. S.V. Patankar, D.K. Basu, and S.A. Alpay, "Prediction of the 3-Dimensional Velocity Field of a Turbulent Deflected Jet," J. Fluids Eng., Vol. 99, p. 758 (1977).

4. G. Bergeles, A.D. Gosman, and B.E. Launder, "The Prediction of Three-Dimensional Discrete-Hole Cooling Processes. Part 1 - Laminar Flow," ASME J. Heat Transfer, Vol. 98c, p. 379 (1976).

5. Patankar, S.V., Pratap, V.S. and Spalding, D.B., 1975, "Prediction of Turbulent Flow in Curved Pipes," J. Fluid Mech., Vol. 67, 583.

6. Pratap, V.S. and Spalding, D.B., 1975, "Numerical Clmputations of the Flow in Curved Ducts," Aero. Quart., Vol. 26, 219.

7. Humphrey, J.A.C., Taylor, A.M.K. and Whitelaw, J.H., "Laminar Flow in a Square Duct of Strong Curvature," J. Fluid Mech., Vol. 83, 509 (1977).

8. Humphrey, J.A.C., "Numerical Calculation of Developing Laminar Flow in Pipes of Arbitrary Curvature Radius," Can. J. Chem. Eng., Vol. 56, 151 (1978).

9. Yee, G. and Humphrey, J.A.C., "Developing Flow and Heat Transfer in Strongly Curved Ducts of Rectangular Cross-Section," LBL Report No. 9092, University of California (1979).

10. Ramos, J.I., Humphrey, J.A.C., and Sirignano, W.A., "Numerical Prediction of Axisymmetric Laminar and Turbulent Flows in Motored Reciprocating Internal Combustion Engines," Proceedings Paper No. 790356, Detroit, Michigan, February (1979).

11. Kreskovsky, J.P., Briley, W.R., and McDonald, H., "Prediction of Laminar and Turbulent Primary and Secondary Flows in Strongly Curved Ducts," Report R80-900007-12, Prepared under contract NAS3-22014 for the NASA-Lewis Research Center, September 1980.

12. Humphrey, J.A.C., "Flow in Ducts with Curvature and Roughness," Ph.D. Thesis, London University, 1977.

13. Pratap, V.S., "Flow and Heat Transfer in Curved Ducts," Ph.D. Thesis, London University, 1975.

14. Leonard, B.P., "A Stable and Accurate Convective Modelling Procedure Based on Quadiatic Upstream Interpolation," Comp. Meths. Appl. Mech. Eng., 19, 59, 1979.

15. Humphrey, J.A.C., Whitelaw, J.H., and Yee, G., "Turbulent Flow in a Square Duct with Strong Curvature," J. Fluid Mech., 103, pp. 443-463, 1981.

16. Gosman, A.D. and Pun, W.M., "Lecture Nores for Course Entitled "Calculation of Recirculating Flows," Imperial College, Mechanical Engineering Report, HTS/74/2, 1974.

17. Launder, B.E. and Spalding, D.B., "The Numerical Computation of Turbulent Flows," Comp. Meths. Appl. Mech. Eng., 3, 269, 1974.

18. Bradshaw, P., "Complex Turbulent Flows," JFE, Trans. ASME, 97, p. 146, 1975.

19. Launder, B.E., "An Improved Algebraic Stress Model of Turbulence," Imperial College, Mechanical Engineering Department Report No. TM/TN/A19, 1971.

20. Rodi, W., "A New Algebraic Relation for Calculating the Reynolds Stresses," ZAMM, 56, T219-221, 1976.

21. Launder, B.E. and Ying, "The Prediction of Flow and Heat Transfer in Ducts of Square Cross-Section," Proc. Inst. Mech. Eng., 187, p. 37, 1973.

22. Tatchell, D.G., "Convection Processes in Confined Three-Dimensonal Boundary Layers," Ph.D. Thesis, University of London, 1975.

23. Melling, A., "Investigation of Flow in Non-Circular Ducts and Other Configurations by laser-Doppler Anemometry," Ph.D. Thesis, University of London, 1975.

24. Buggeln, R.C., Briley, W.R., and McDonald, H., "Computation of Laminar and Turbulent Flow in Curved Ducts, Channels, and Pipes Using the Navier-Stokes Equations," Final REport to the Office of Naval Research, Report R80-920006-F, December 1980.

25. Ghia, K.N., and Sokhey, J.S., "Laminar Incompressible Viscous Flow in Curved Ducts of Rectangular Cross-Section," JFE, Trans. ASME, 99, pp. 640-648, 1977.

26. Yee, G., Chilukuri, R., and Humphrey, J.A.C., "Developing Flow and Heat Transfer in Strongly Curved Ducts of Rectangular Cross-Section," JHT, Trans. ASME, 102, pp. 285-291, 1980.

27. Bergeles, G., "Three-Dimensional Discrete-Hole Cooling Processes. An Experimental and Theoretical Study," Ph.D. Thesis, London University, 1976.

APPENDIX 1

CONSTRUCTION AND VALIDATION OF A CURVED DUCT EXPERIMENTAL FLOW SYSTEM AND ITS ASSOCIATED MEASUREMENT INSTRUMENTATION*

by

G.M. Beshouri[1] and J.A.C. Humphrey[2]

Department of Mechanical Engineering
University of Caliornia
Berkeley, CA 94720

INTERIM REPORT OF EXPERIMENTAL WORK
CONDUCTED FOR NSF UNDER GRANT NO. ENG-78-27007

AUGUST 1980

---

* The bulk of this document is based on the Project Report submitted by the first author in partial fulfillment of the requirements for the Degree of Master of Science at UC Berkeley.

[1] Graduate research student

[2] Assistant Professor,
Principal Investigator

CONTENTS

ABSTRACT

Turbulent flows arise in numerous engineering applications involving the transport of fluids such as are found in heat exchangers, chemical reactors and intake ducting to gas turbines, to name a few. Numerical schemes exist which purport to model such flows, and they require verification. By using laser Doppler anemometry (LDA), experimental data for turbulent flow in a sharply curved duct can be obtained, which will help to verify turbulence models for this special case of flow. This report discusses the construction and initial testing of an experimental apparatus and associated electronic instrumentation to be used in an on-going investigation of curved duct flow.

INTRODUCTION

Turbulent flow commonly occurs in many industrial applications. Often little detailed knowledge of the flow is required, knowledge of the pressure drop sufficing. However,some cases such as intake ducting to gas turbine engines, chemical reactors and heat exchangers require more detailed information. Obtaining this information experimentally requires considerable time and expense. Numerical methods for predicting such flows exist which could also be used, at much less cost. However, the reliability of such methods must be verified.and experimental data which allows such verification is therefore desirable.

This report describes part of a project concerned with providing such experimental verification utilizing laser Doppler anemometry to measure turbulent flow in a sharply curved duct of square cross section. Specifically, the report describes in detail the experimental apparatus, the LDA system and the computer interface. Preliminary results are also included to show that the system as a unit functions and can provide accurate data. The unit as a whole will be used in an on-going investigation pertaining to turbulent flow in curved duct.

EXPERIMENTAL APPARATUS

This section contains a detailed description of the experimental apparatus including the flow system, test section, bulk flow measurement and valving, and plumbing. A brief description of the system in operation is also included.

Flow System

The basic flow system is shown in Figures 1-a and b. It consists of a plexiglass test section connected to an elevated head tank in which a constant head of water is maintained, a large reservoir, a venturi meter connected to a mercury manometer to measure bulk flow, a centrifugal pump to feed the head tank from the reservoir, and associated valving and plumbing trhoughout the system. Unless otherwise noted the "test section", shown in Figure 2, consists of the whole of the plexiglass unit including the curved section, the upstream and downstream tangents and a flow straightener (to be described).

Figures 3a and b are drawings of the flow system with relevant dimensions indicated. The reservoir consists of a 4 x 4 x 4 ft^3 (1.2 x 1.2 x 1.2m^3) tank constructed of 0.080 in. (2.0 mm) galvanized steel, coated with a silicone rubber sealer for added protection against corrosion at the weld joints. The head tank is 2 x 2 x 2 ft^3 (0.6 x 0.6 x 0.6 m^3) and of similar construction. A Unistrut steel structure supports the head tank above the reservoir, with a distance of 10 ft. 4 in (3.14 m) from the bottom of the reservoir to the top of the head tank.

Pumping is performed by a Burkes centrifugal unit (P.N. 7-G-1¼, C.N. 765-1) consisting of a 4.5 in (11.4 cm) impeller with a 1 1/4 in (3.18 cm) outlet driven by a manufacturer fitted 3/4 HP A.C. motor. The pump inlet connects to the base of the reservoir so that it self-primes. The connection is made with

1.5 in sched. 80 P.V.C. pipe with two ball valves between the pump and reservoir to prevent backflow and to facilitate maintenance. Similar piping extends from the pump outlet to a gate valve operated as a throttle and then up and over the lip of the head tank and into the tank itself. The pipe outlet is horizontal, 4 in (10 cm) above the bottom of the tank, 1.5 in (3.8 cm) from the left wall, 4 in (10 cm) from the front wall and at a 45° angle to those walls. This geometry creates a gentle three dimensional swirl in the head tank allowing the flow to rise to the surface thus purging any air entrained before leaving the head tank for the test section.

Water discharges from the head tank through two outlets in the bottom. A 17 in (43 cm) section of 2.4 in sched. 80 P.V.C. pipe extends into the head tank from one outlet to provide the constant head. The other side of this outlet connects to similar pipe which extends down to 8 in (20 cm) above the bottom of the reservoir. A 12 in (30.5 cm) diameter plexiglass plate held at 45° from the bottom of the tank deflects the overflow from this pipe away from the pump inlet to minimize possible air entrainment.

An 8 in (20 cm) tall, 5.5 in (14 cm) inside diameter, 6.5 in (17 cm) outside diameter plexiglass cylinder, with a galvanized steel mesh covering the end, extends above the second outlet. This device serves to break up any vortices which might entrain air and/or create a fluctuating head in the test section. A 2 in I.D. 32 in (81 cm) long brass tube extends from this outlet and attaches to a 2 in I.D. 52 in (132 cm) long tygon tube which in turn connects to the test section entrance flow control valve (see Figure 4).

A tee ball valve and a 6 in (15 cm) long pipe which discharges 9 in (23 cm) above the lip of the reservoir is plumbed into the piping extending from the pump to the head tank. This valve operated as a bleed until a throttle valve

was placed on the pump. It now serves to drain the head tank if it is impossible to drain it through the test section according to normal procedure. During normal operation this valve is closed and not used.

Test Section

As stated above, the test section consists of a curved section with upstream and downstream tangents and a straightening section connected to the upstream tangent. The curved part of the test section (see Figure 5) was constructed from clear plexiglass. One solid piece 3 in (7.6 cm) thick was machined to give a square cross section channel of 1.75 x 1.75 in ^{2} (4.45 x 4.45 cm^2) with a mean radius of 5.875 in (14.92 cm) over an arc of 180°. A plexiglass plate 0.5 in (1.3 cm) thick was machined to fit over the open channel and is held in place by brass machine screws thus yielding the enclosed curved duct geometry of interest to this work. An o-ring seal between the two plexiglass pieces ensuresthat the curved test section is leak-proof during operation. The hydraulic diameter D_H is equal to that of the straight ducts (1.75 in)4.45 cm) and the curvature ratio $R_c/D_H/2$ is equal to 5.7. The outer radius wall of the curved channel is formed by a 0.0625 in (1.599 mm) thick, curved stainless steel sheet. There are four sector shaped compartments constructed of plexiglass on the outer side of this stainless steel wall. Hot fluid pumped through these compartments, or electric heaters,can provide heat transfer through the stainless steel wall to the flow for future experiments.

The tangent sections (see Figure 6) are each 55 in; (190 cm) long corresponding to 31.4 hydraulic diameters, with the same cross section as the curved duct. With the flow straightener attached, the upstream tangent ensures fully developed flow at the curved duct. The downstream tangent serves to avoid upstream propagation of disturbances from the downstream flow. Like the curved duct, the

tangents were constructed from 0.5 in (1.3 cm) thick transparent plexiglass.

The flow straightening section (shown in Figure 5) is 12.5 in (31.8 cm) long corresponding to 7.15 hydraulic diameters. This section contains three removable plates. Each plate is a 0.125 in (3.175 mm) thick piece of plexiglass containing 85 - 0.125 in (3.175 mm) diameter holes drilled in a rectangular array spaced 0.177 in (4.495 mm) on centers in each direction. A plate is placed 0.75 in (1.905 cm) from the inlet and another at the outlet of the section, with the remaining plate in the middle 5.5 in (14.0 cm) from each of the others. The perforated plates serve to homogenize the flow. They also promote rapid transition to a turbulent flow condition in the upstream tangent. A 5 in (12.7 cm) long 1 cm pitch section of aluminum honeycomb placed between the first and second plates serves to break up weak secondary motions introduced by the section of curved tygon tube between the constant head tank and the test section. The entire straightener is constructed of plexiglass.

All machined plexiglass surfaces have tolerances of ± 0.005 *in* (0.127 *mm*). All walls of the tangent sections and the straightening section are glued together, as are the heating chamber dividers. The top walls of the curved and straightening sections are removable, and fastened with brass machine screws. O-rings are used to seal the removable walls and the flanges connecting the sections. The sections are bolted together at the flanges using brass machine screws and nuts. A 2 in outside diameter, 2.5 in (6.35 cm) long plexiglass tube is glued to the inlet side of the flow straightener and the outlet side of the downstream tangent. This provides an attachment point to connect the test section to the rest of the flow system.

Bulk Flow Measurement

A 2in Barco venturi meter (P.N. 2-393), which is accurate to ± 2% over a range of 6-60 G.P.M. (22.7 - 230 ℓ/min), measures the bulk flow. The venturi meter is connected to a 50 in (1.27 m) differential manometer filled with mercury. The mean velocity of the flow in the test section is determined from the expression:

$$V = 0.4092\ [\Delta P]^{1/2}$$

with V = velocity in meters/second and ΔP = pressure drop in inches of mercury. The Reynolds number may similarly be determined from the expression:

$$Re = 1.718 \times 10^4\ [\Delta P]^{1/2} \quad .$$

Valving and Plumbing

The outlet side of the tygon tube from the head tank connects to a brass adaptor followed by a 2 in bronze gate valve. This valve serves as the throttle for the test section and is followed by a 4 in (10 cm) section of 2 in brass pipe connected to a 2 in P.V.C. union. Another brass adaptor connects the union to a 6 in (15 cm) piece of 2in inside diameter tygon tube attached to the inlet plexiglass tube of the flow straightener. At the outlet side of the downstream tangent, a similar tygon tube - adaptor union arrangement is followed by a 13 in (33 cm, 6.5 D_H) section of 2 in diameter brass pipe connected to the venturi inlet. The outlet side of the venturi is connected to a 6 in (15 cm, $3D_H$) long, 2 in brass pipe followed by a 2 in bronze ball valve which is used when purging air from the manometer leads. An 8 in (20 cm) section of 2 in brass pipe follows which connects to 2 in inside diameter tygon tube which enters the reservoir through a hole in the front of the tank above the water level and then discharges below the water level. This tygon tube is securely clamped to the Unistrut structure supporting

the head tank to prevent any oscillations in the tube which might propagate back into the test section.

The test section, plumbing, valving and venturimeter are securely mounted to a table constructed from steel Unistrut. This table is securely clamped to the floor by four 0.5 in. steel bolts to minimize oscillations. Provision is made to level the table. When mounted on the table the top of the test section is 31 in (79 cm) above the floor.

Operation

In operation mode the reservoir is filled to the 2 ft (61 cm) mark yielding an overall head of 7ft 9 in (2.36 m). Water is pumped from the reservoir into the head tank at a rate of 50-60 G.P.M. (190 - 230 ℓ/min) at wide open throttle. Part of this flow (33 G.P.M., 125 ℓ/min at wide open throttle) empties through the outlet leading to the test section. After flowing through the test section this water discharges back into the reservoir and continues the cycle. That portion of the flow into the head tank which does not enter the test section spills into the reservoir through the overflow outlet.

LDA MEASUREMENT INSTRUMENTATION

This section contains a description of the laser-Doppler anemometer including mounting and traversing hardware, the optical components, mirrors and related instrumentation.

Traversing Mechanism

The laser-Doppler anemometer (LDA) system is shown in Figures 7 and 8. It consists of a Lexel 2 Watt Argon Ion two color (green - 514.5 nm and blue - 488.0 nm) water cooled laser, a mirror stage (shown in Figures 9a, b) for reflecting the laser beam into the anemometer optics, the anemometer optics (described below), and a 4 in (10.2 cm) diameter mirror for reflecting the anemometer beams from the horizontal to the vertical direction and for collecting backscatter radiation to measure two velocity components in the curved duct.

The laser, mirrors and optics are mounted to the top of a 0.50 in (1.27 cm) thick aluminum table which is itself firmly bolted to an X,Y,Z traversing mechanism. The traversing mechanism is positioned by three stepping motors with linear encoders which are controlled and monitored by a PDP 11/34 computer. Thus, after displacement of the traversing mechanism in any direction the new position of the measurement volumne, relative to a fixed reference point, is known to within 5 microns. Along any coordinate direction the traversing mechanism can be displaced up to 6 in. (15.2 cm).

Castors are mounted on the bottom of the traversing mechanism to allow coarse manual placement of the optical instrumentation relative to the test section. Once this placement is made, the unit is raised on four bolts acting as levelling screw jacks, so that the optics are firmly fixed relative to the test section. Fine adjustments with the stepping motors are then made to obtain the exact required orientation of the control volume.

Optical Components

The LDA optical components, manufactured by Disa Electronics (series 55X) consist of:

55 x 12 beam expander

55 x 20 cover and retarder

55 x 23 support

55 x 25 beam splitter

55 x 27 beam splitter

55 x 29 bragg cell*

55 x 30 backscatter section

55 x 31 pinhole section

55 x 32 beam translator

55 x 34 optics

55 x 35 color separator

55 x 51 300 mm front lens.

Two RCA-4526 photo multiplier (P.M.) tubes were purchased from Disa but P.M. tube housings and the associated electronics were constructed and assembled by the machine and electronics shops. One of these P.M. tube housings is shown mounted on the optics in Figure 7.

The entire LDA system was assembled in backscatter mode (the same optical components can be assembled in forwardscatter mode). This arrangement is advantageous in systems such as the present one where it is desirable to produce measurement volume displacements without causing optical misalignment. The availability of a powerful laser source and the relative abundance of adequately scattering particles in the water flow facilitate backscatter anemometry. The advantages and disadvantages of forward and backward scattering LDA systems will be found discussed in more detail in [1].

* In this work the Bragg cell frequency shifter was not used in conjunction with the rest of the LDA optical components since reversed flow regions were not anticipated at the location where measurements were made.

The characteristic dimensions of the measurement volume produced by the 55 x 12 beam expander in conjunction with a 310 mm focal length lens, with beams intersecting at a half angle of 3.28° are: length = 1.6 mm, diameter = 100 μm. The number of fringes produced in the measurement volume were approximately N_f = 100. However, spatial filtering and a threshold setting on the counter reduced the number of fringes for signal measurement to between 10 - 20.

Mirrors

The mirror stage for reflecting the laser beam into the LDA optical components is shown in Figures 7, 9a and 9b.

This component allows a reduction in the table length required to support the laser and LDA optical components by permitting them to be mounted side-by-side instead of in tandem. The mirror stage consists of three mirror assemblies mounted to two parallel 17.68 x 6.5 x 0.75 in (44.9 x 16.5 x 0.56 cm) aluminum plates held 12 in (30.5 cm) apart by 2-1.5 in (3.8 cm) and 2-0.75 in (1.9 cm) diameter aluminum bars. Each mirror assembly consists of a Newport Research Corporation (NRC) manufactured 1 in (2.5 cm) diameter mirror* glued to an adjustable NRC mirror mount (P.N. MM-2) which is attached to an adjustable 2.75 x 1.5 x 0.5 in (7.0 x 3.8 x 1.3 cm) aluminum stand. One mirror assembly is mounted directly to the lower plate. The other two assemblies are bolted to NRC translation stages (P.N. 420-05) which are both mounted to the upper plate.

The horizontal beam from the laser is deflected up 90° by the lower mirror. The next mirror deflects this beam another 90° back to the horizontal, and the third mirror deflects the beam over another 90° in the horizontal plane. The net result is a beam that is parallel to the emitted beam shifted 11.25 in

* The mirrors consist of a pyrex glass substrate with a dielectric multilayer coating optimized to reflect the light at an incidence angle of 45° (P.N. 10 D20 DM.2).

(28.6 cm) over and 9 in (22.9 cm) up, travelling in the opposite direction. Various adjustments are required for accurate positioning of the beam along the optical axis. A relatively hefty construction of the stage unit is required to minimize sensitivity to externally imposed vibrations. All aluminum parts were anodized black.

The anemometer beams leaving the optics are deflected into the test section by a 4 in. (10.2 cm) diameter glass-silvered mirror (see Figures 7 and 8) which also reflects the backscatter radiation back into the optics. The mirror is held in an NRC post-mounted adjustable mirror mount (P.N. 625A-4), which is supported by two perpendicular 1.5 in (3.8 cm) diameter aluminum posts. The vertical post is fixed in an annular receptacle built into the optics table, and the horizontal bar is clamped to it by means of an adjustable aluminum sleeve. As with the mirror stage, heavy structural components were utilized to minimize vibration. All aluminum parts were anodized black.

Operation

A brief description of the operation of the LDA system follows.

Light emitted by the laser is circularly polarized by the Cover and then passes through the mirror stage. It then enters the first component of the optics, the Retarder, where the circularly polarized light is again linearly polarized. The beam is then split 50:50 by the (neutral) Beam Splitter and next enters the color Beam Splitter where one of the beams is separated 50:50 into blue and green beams. These three beams then pass through the outside of the pinhole section and into the Translator where the relative position of the beams can be adjusted to obtain optimum fringe spacing. The beams next pass through the Expander, allowing the measurement volume to be decreased which increases the intensity of the collected light thereby improving the signal to noise ratio. The beams then pass through a convex lens which

focuses them into a measurement or "control" volume. The 4 in diameter mirror deflects these focused beams into the test section.

The light scattered by particles in the flow is reflected by the same 4 in mirror back through the lens and down the pinhole which acts as a spatial filter to eliminate undesirable reflections or scattered light. This light is then reflected by a mirror in the backscatter section into the P.M. optics, then through a color separator and then blue and green filters. The separated blue and green light enters respective P.M. tubes where an electrical signal is generated. These signals are fed in parallel* to separate Disa 55L96 LDA counters which validate, filter and amplify the Doppler signals and then translate their frequency content into a digital output which is input to the PDP 11/34 (see next section).

Characteristics of the Disa counters used in this work are available in [2]. For more detailed descriptions relating to the use of counters in LDA systems see [3]. For a more detailed discussion of the LDA technique see [1].

* In this work measurements were only made of one component of velocity, with the green (514.4 nm) radiation.

DATA ACQUISITION AND PROCESSING SYSTEM

This section contains an outline of the PDP 11/34 minicomputer and the data acquisition methodology. For a more detailed description of the computer system and data acquisition see [4].

The PDP 11/34 Computer

The PDP 11/34 computer, manufactured by Digital Equipment Corporation, acts as the central data acquisition and reduction controller, and processor. It has a 34K 16 bit word memory and is equipped with dual removable RL01 disc drives (5 Mbytes each) and dual double density Floppy diskette drives (500 K Mbytes each). The minicomputer interacts through a number of interface options with external devices under a real time 11 software package as shown in Figure 10. Available input-output devices include a Tektronix 4025 graphics terminal, a Decwriter II hardcopy terminal and a Tektronix 4662 digital pen plotter (see Figure 13).

Data Acquisition

A handshake technique was employed for data acquisition whereby a logic conversion circuit conditioned the lines from the Disa LDA counter to the DR11-L parallel line interface module. At every validation of a Doppler burst a "data ready" signal was issued by the counter for the logic conversion circuit. This circuit then sent a triggering pulse to the computer interface which was checked for data availability by a software loop approximately every 20 microseconds. No interrupt routines were used for obtaining data due to the higher sample rates made possible by the handshake technique.

RESULTS AND DISCUSSION

In this section some preliminary measurements are provided for the longitudinal mean velocity and turbulence intensity at a station two hydraulic diameters into the downstream tangent where the influence of the curved section on the flow should still be noticeable. The main purpose in making the measurements was to show that the laser-Doppler anemometer and the minicomputer were functioning properly, and to validate the software controlling the entire measurement operation. This software package has been documented in [5] and is briefly outlined below.

The measurement procedure was at follows. The optical system was first carefully aligned relative to the duct measurement station, and it was verified that displacements of the LDA by the traversing mechanism did not cause misalignment. A reference point was then chosen on one of the corners on the inside of the downstream tangent and was labelled X=0, Y=0, Z=0. All subsequent traversing was controlled by software instructions relative to the zeroed point. Instructions were given via the Tektronix 4025 graphics terminal to the software package, indicating the initial and final coordinate positions to be probed by the measurement volume, the order in which the coordinate axes should be followed and the ΔX, ΔY, ΔZ increments to be taken. Various system constants and additional parameters, such as the number of data points to be taken per position in the flow were also read into the software package. In the present work 10 measurements were made per position and each one of these was based on 1000 validated Doppler bursts.

Before the experimental run the counter was fixed to the following control settings: combined 5/8 and variable fringe number operation mode, 6% comparator accur low pass filter set at1 kHZ, high pass filter set at 64 kHZ. Optimal conditioning of the signal was achieved by setting the amplifier gain and threshold window to

appropriate levels. An indication of the quality of the Doppler bursts was observed by displaying the signals on a Tektronix 5440 Scope. Data rates of about 1 kHZ, with approximately 60% validation, provided a further indication of the high quality of the data.

Upon activation of the software package the minicomputer took control of the entire measurement sequence. The validated data was temporarily stored in arrays which were subsequently processed by a statistical routine in the software package to yield a mean value and the standard deviation of the 1000 observations per measurement. Two traverses were made of 20 points each to check the automatic data aquisition sequence. (For a sample of typical output, see Table 1).

At each of the points in the traverse 10 values of the mean velocity and turbulence intensity were determined. Figures 11 and 12 show plots of the averages of these measurements. The size of the points provides an indication of the error in the measurements. While the physical meaning of the results is not entirely clear the collection of these results serves as confirmation of the performance of the automatic data acquisition system. Of course, further testing is required of the system for its complete validation, but the present results are very encouraging.

The plots shown in Figures 11 and 12 are not devoid of physical meaning. The profiles were taken at approximately equal distances from the symmetry plane in the flow. The precise locations are shown as dotted lines in the squares on the respective figures. Inspection of the nondimensional velocity measurements shows the flow moving more quickly at high values of X/D (corresponding to the outer radius wall in the curved section). The more striking feature of the data is contained in the profiles for turbulence intensity. These show high turbulence activity at the side walls of the downstream tangent but with higher levels at

low values of X/D (corresponding to the inner radius wall in the curved section). The latter result suggests that high levels of turbulence activity are being produced at the inner walls of the curved section which are then convected into the downstream tangent by the bulk flow. Both figures show a peak in the turbulence intensity for $0.25 \lesssim X/D \lesssim 0.50$. Given the relative precision in $\tilde{u}_y$ ($\lesssim$ 5% for the data plotted) it is believed that the peaks represent a region of strong shear in the flow. This is supported by corresponding pronounced variations in the plots for U_y at approximately the same locations. The data is, of course, too sparse to allow definite conclusions to be drawn regarding specific characteristics of the flow. Further and considerably more detailed experimentation is required.

CONCLUSIONS

An apparatus has been constructed for the experimental investigation of square cross-section curved duct flow with long tangents attached.

A laser Doppler anemometer of Disa manufacture capable of making simultaneous measurements of two velocity components in backscatter mode was assembled. The instrumentation required various modifications to make data aquisition feasible in a fairly compact space. This was achieved by means of two mirror stages which were specifically designed for this purpose.

The main features of the mini-computer - LDA automatic data acquisition system have been tested and validated. The tests included checking that the traversing mechanism responded accurately to displacement instructions given by the computer and that data validated on the counter was accepted and subsequently reduced correctly by the computer. To this end a software package described in [5], used to control the entire experimental sequence, was debugged and implemented satisfactorily. Further extension of the system from one to two velocity component measurements remains to be done.*

Preliminary measurements at a station downstream of the curved section were obtained and are the basis for concluding that the automatic data aquisition system is working properly. The data show physically plausible and interesting characteristics. A detailed investigation of the mean and turbulence characteristics of the flow are now required.

---

* This is in the process of being concluded.

ACKNOWLEDGEMENTS

Funding for this work was provided by the National Science Foundation through Grant No. 442447-21895-R.

We gratefully acknowledge the considerable assistance and expertise provided by Mr. George Lewis and Mr. Wes Lim in constructing the experimental apparatus and electronic instrumentation respectively. Special thanks are due to Dr. A. Modavi who was instrumental in the design and implementation of the automatic data aquisition system. Thanks go to S. Li, R. Chilukuri and N. Al-Shama who participated in various aspects of the initial design of the experimental test section and to Mr. L. Grout and W. Gandola for its construction.

REFERENCES

1. L.E. Drain, The Laser Doppler Technique, Wiley, 1980.

2. Disa 55L90A LDA Counter Processor, Disa Information Department.

3. F. Durst, A. Melling and J.H. Whitelaw, Principles and Practices of Laser Doppler Anemometry, Academic Press, 1976.

4. A. Modavi, to appear as an LBL Report, 1980.

5. A. Modavi, to appear as an LBL Report, 1980.

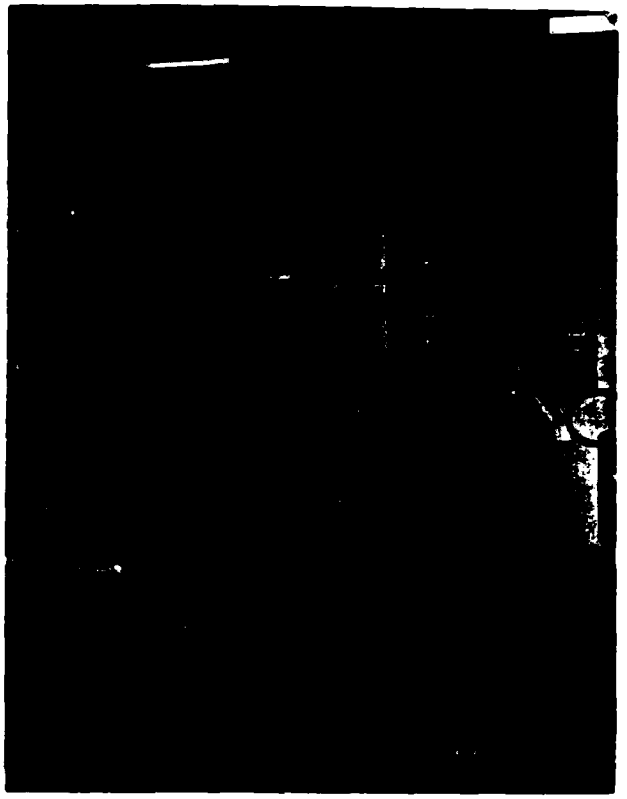

Figure 1a: View of flow system: plexiglass test section, sump and constant head tanks.

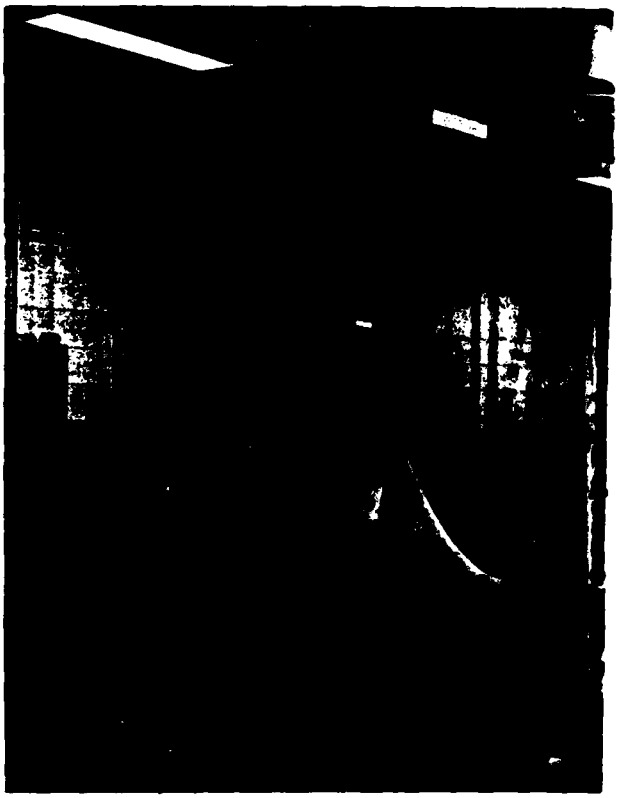

Figure 1b: View of flow system:centrifugal pump, sump and constant head tanks.

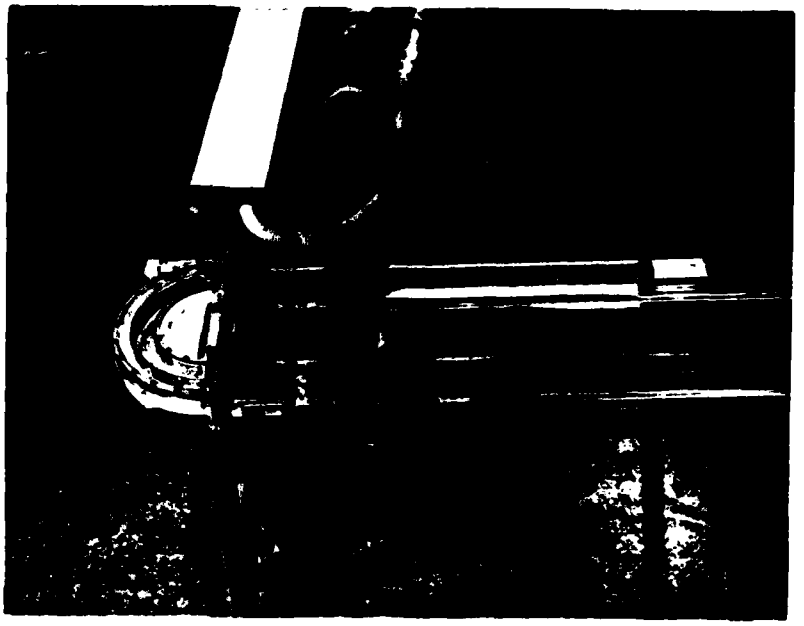

Figure 2: Transparent experimental test sections: 180 degree curved duct of square cross-section with straight tangents attached. Part of the laser-Doppler anemometer optics are shown resting on the X,Y,Z traversing mechanism.

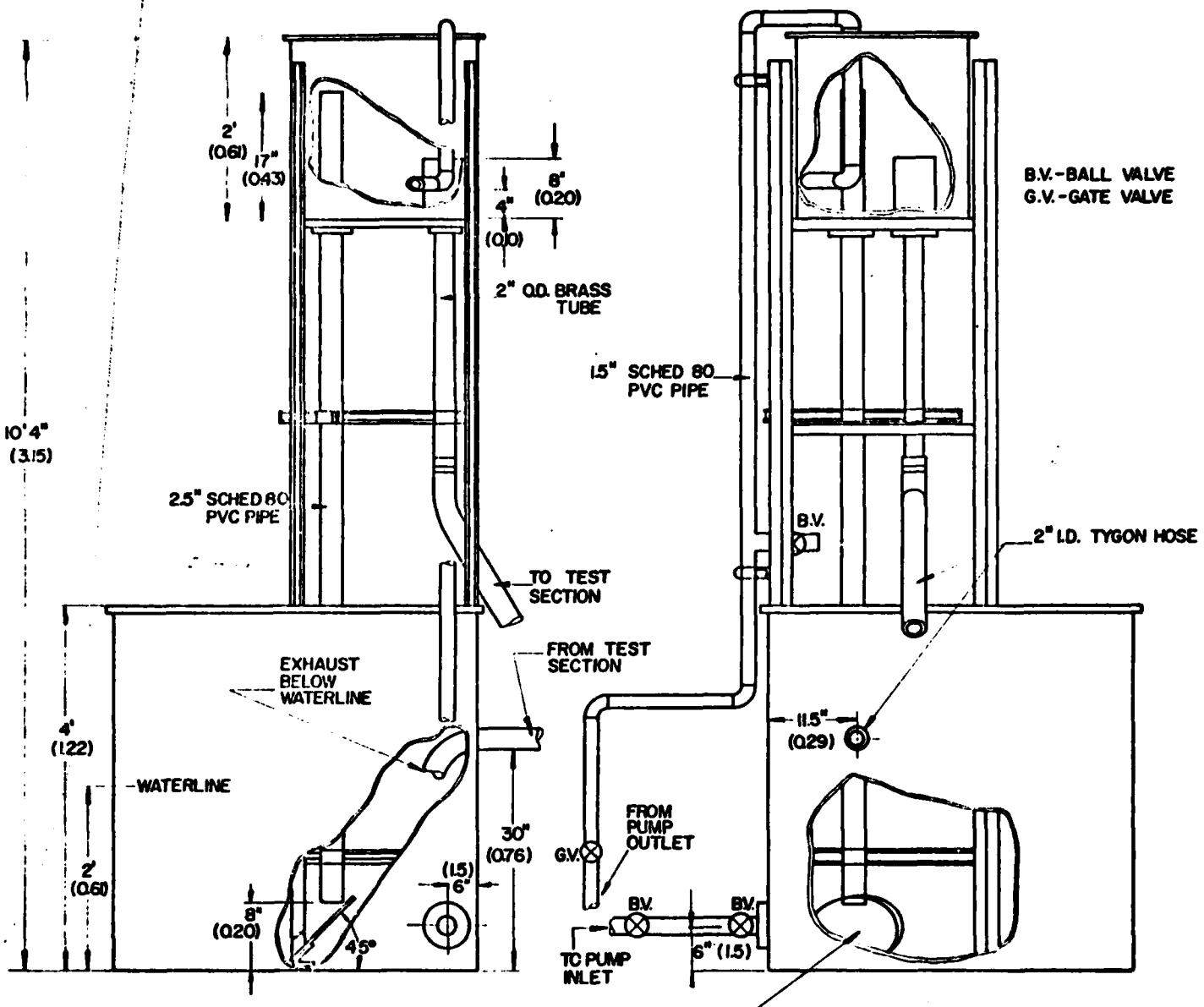

Figure 3a: Front and side views of flow system.

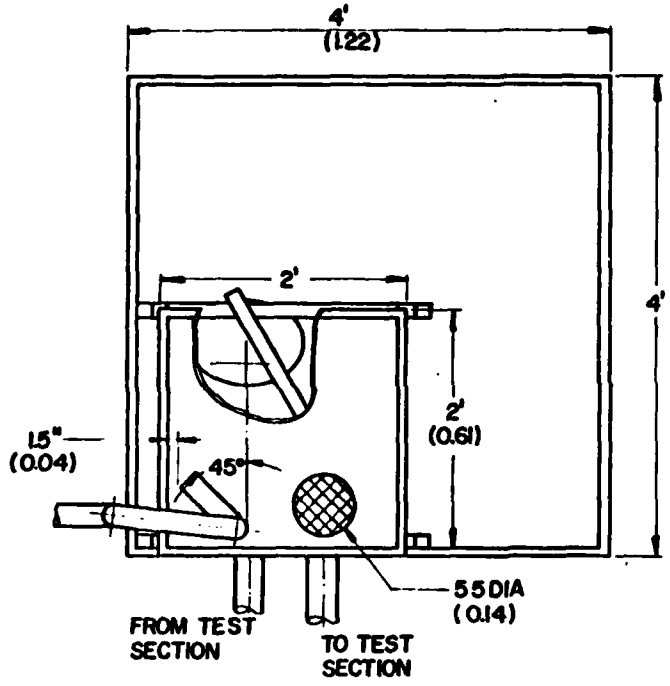

Figure 3b: Top view of flow system.

SCALE: 1" = 1'

(DIMENSIONS IN BRACKETS ARE IN METERS)

Figure 4: Entrance and exit tangent connections to the flow system. Venturi meter and on-off valve are shown connected to the downstream tangents. Tygon tubing and a gate-valve are shown connected to the flow straightening section attached to the upstream tangent.

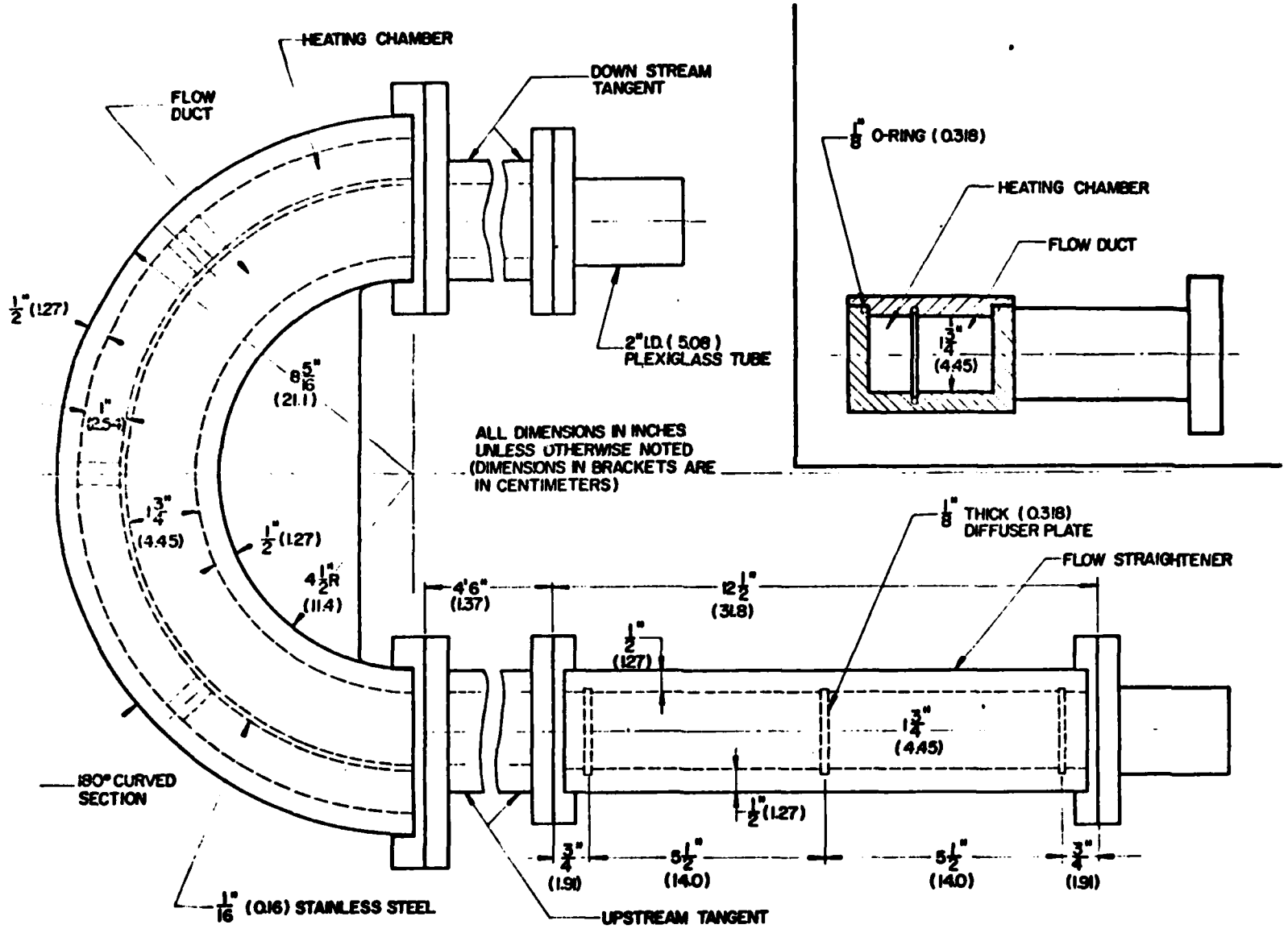

Figure 5: Detailed view of flow test section.
Insert shows cross-section at 90 degrees.

SCALE: 1" = 1'
(DIMENSIONS IN BRACKETS ARE IN METERS)

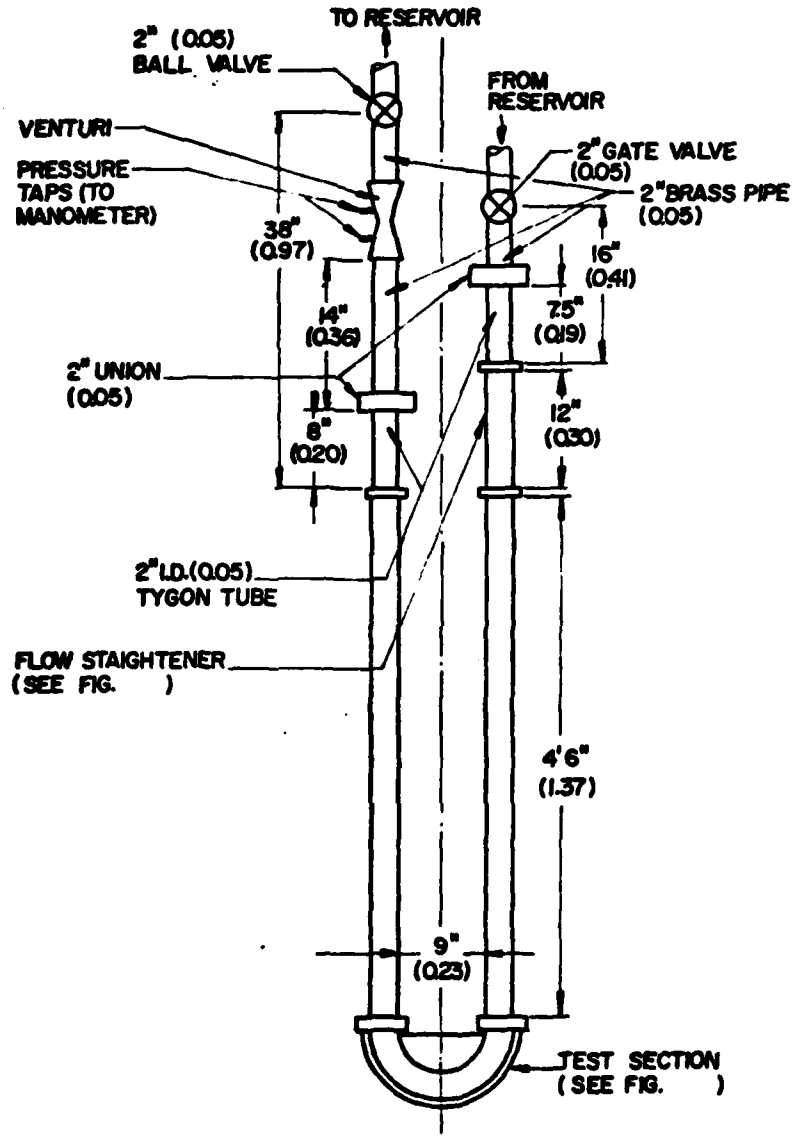

Figure 6: Schematic of flow test section with dimensions indicated.

SCALE: 1" = 1'

(DIMENSIONS IN BRACKETS ARE IN METERS)

Figure 7: Laser-Doppler anemometer supported on motored and encoded X,Y,Z traversing mechanism. Plastic hose resting on table provides coolant water to a 2 W Lexel Argon Ion laser. Test section shown to left of photograph.

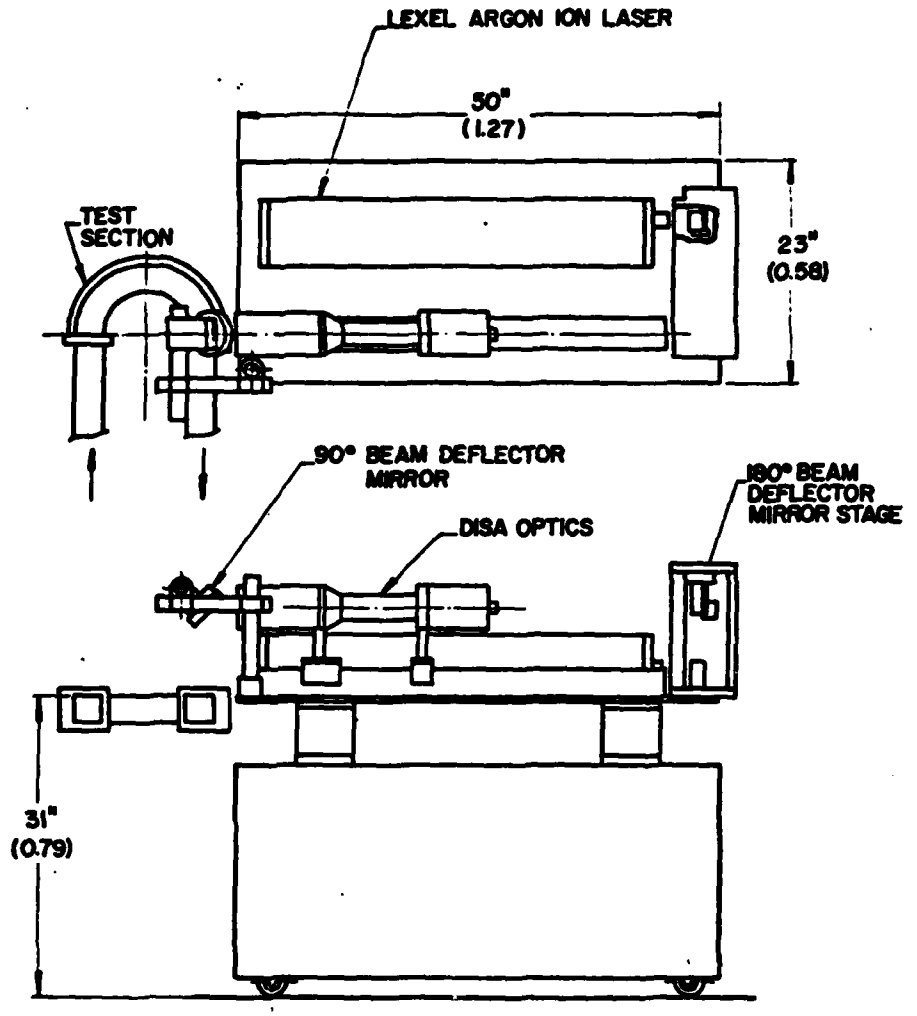

Figure 8: Top and side view of laser-Doppler anemometer and X,Y,Z traversing mechanism in relation to the flow test section.

SCALE 1" = 1'

(DIMENSIONS IN BRACKETS ARE IN METERS)

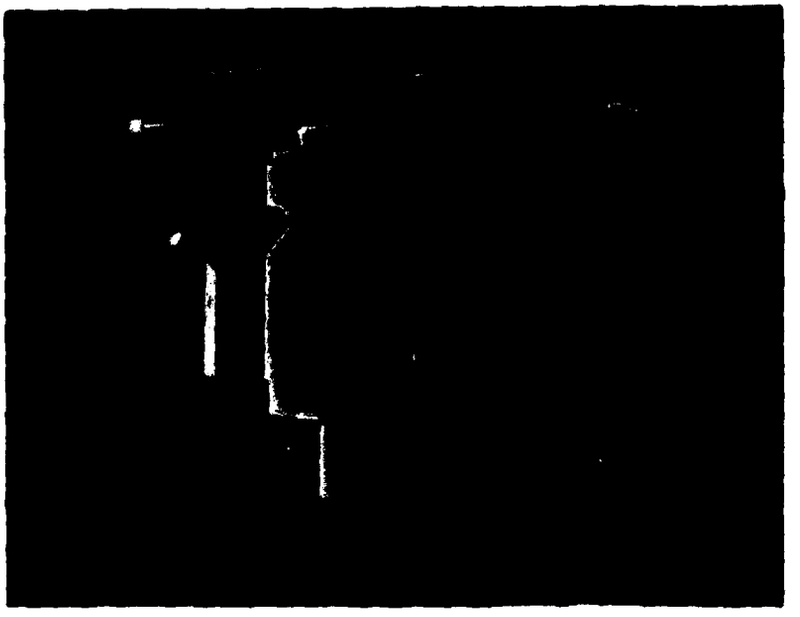

Figure 9: Two views of 180 degree beam deflecting mirror stage.

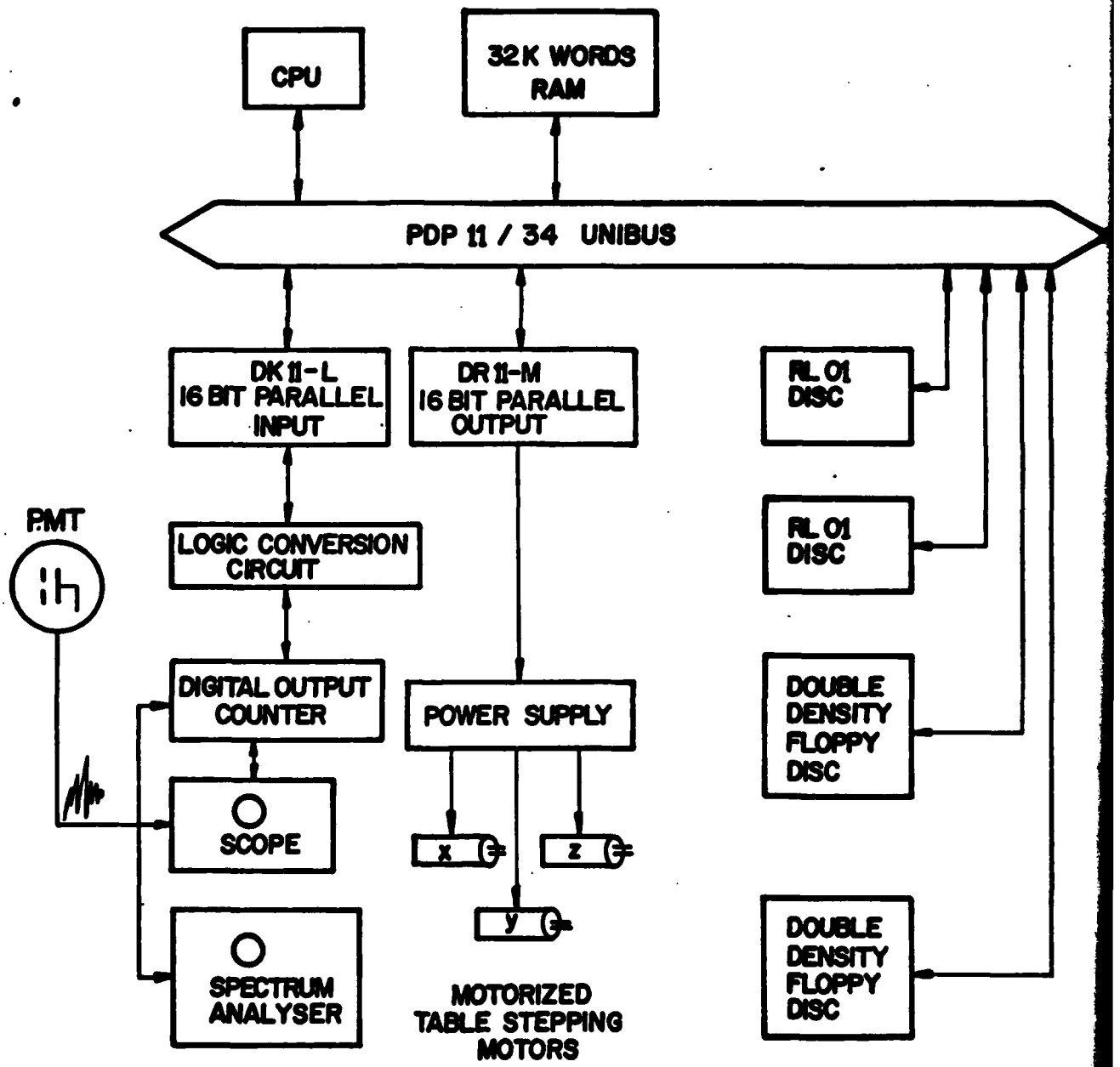

Figure 10: Laser-Doppler velocimeter - PDP 11/34 interface.

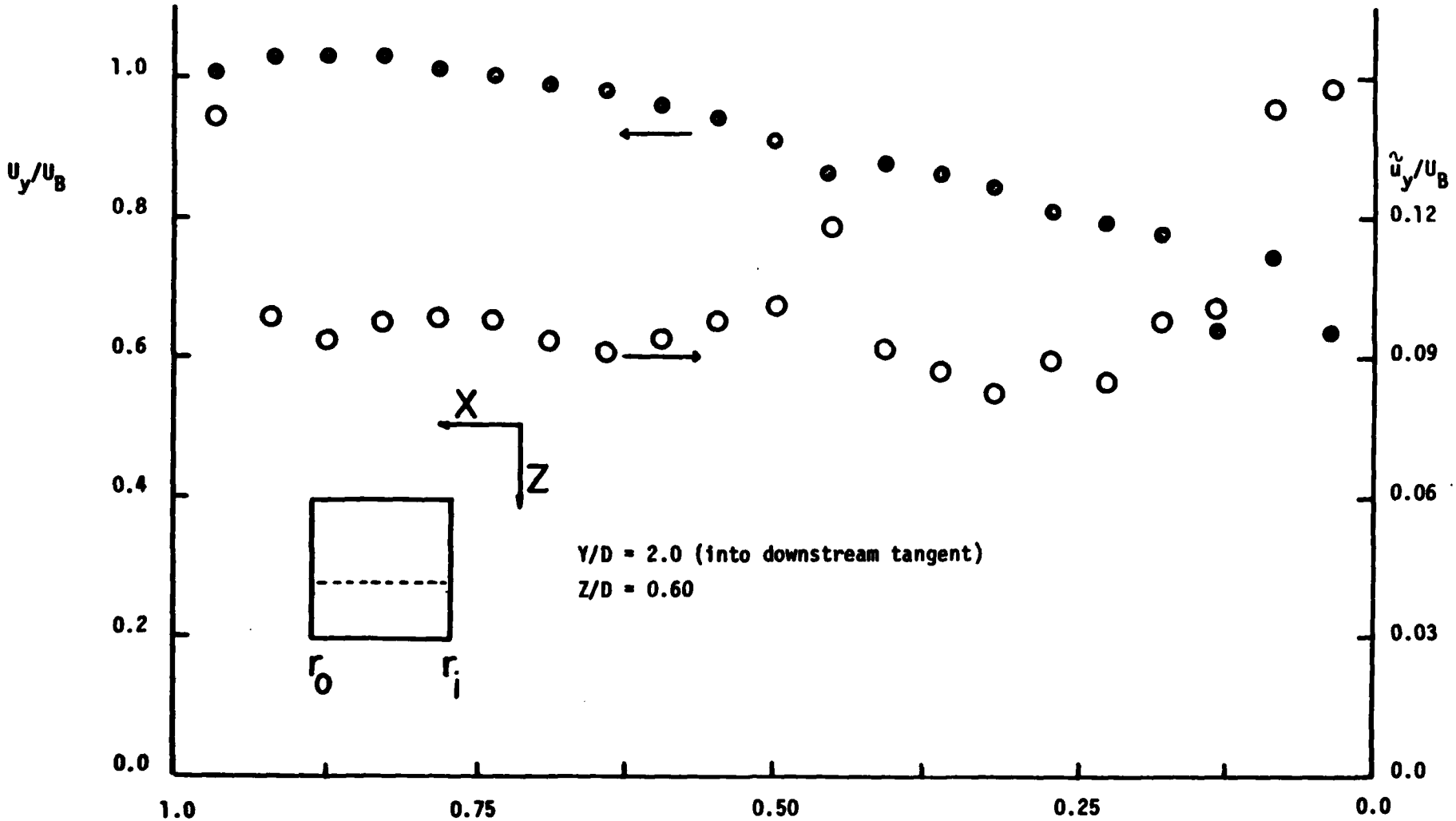

Figure 11: Mean velocity and turbulence intensity normalized by bulk velocity for conditions shown.

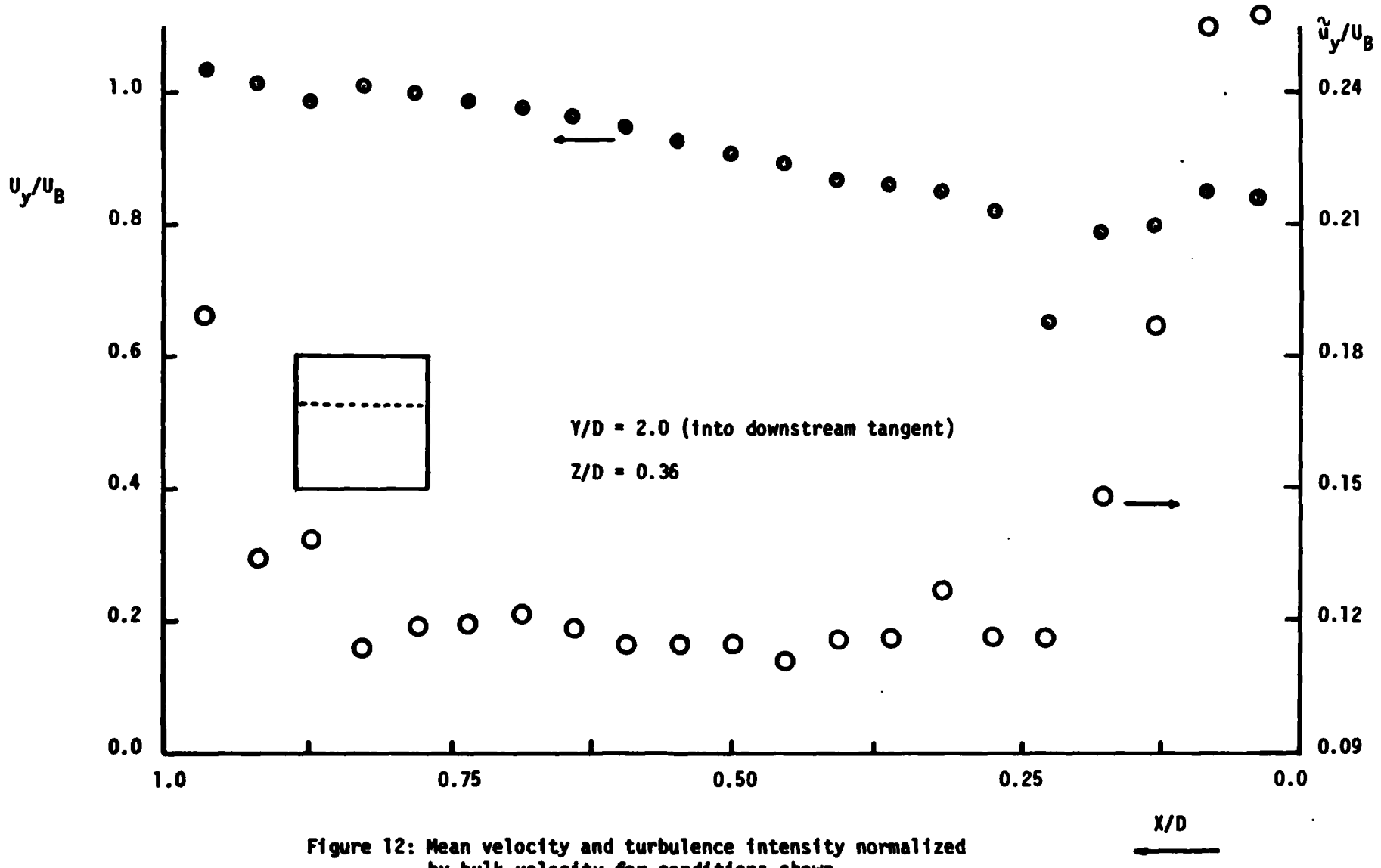

Figure 12: Mean velocity and turbulence intensity normalized by bulk velocity for conditions shown.

Figure 13: Computerized data acquisition system electronic instrumentation. From left to right are shown: Tektronix 4025 Graphics Ter., PDP 11/34 minicomputer, DISA 55L96a counters, frequency shifter downmixers and photomultiplier tube power supply, Decwriter II hardcopy terminal,Tektronix 5440 Oscilloscope.

X	Y	Z	POP	UMEAN	UMS	URMS	UTI
1.500	0.000	11.500	1	0.1063E+01	0.2872E-01	0.1695E+00	0.1650E+02
1.500	0.000	11.500	2	0.1063E+01	0.3554E-01	0.1885E+00	0.1836E+02
1.500	0.000	11.500	3	0.1076E+01	0.4097E-01	0.2024E+00	0.1971E+02
1.500	0.000	11.500	4	0.1074E+01	0.3815E-01	0.1901E+00	0.1851E+02
1.500	0.000	11.500	5	0.1071E+01	0.3799E-01	0.1949E+00	0.1898E+02
1.500	0.000	11.500	6	0.1085E+01	0.4341E-01	0.2084E+00	0.2029E+02
1.500	0.000	11.500	7	0.1083E+01	0.3895E-01	0.1974E+00	0.1922E+02
1.500	0.000	11.500	8	0.1070E+01	0.3812E-01	0.1952E+00	0.1901E+02
1.500	0.000	11.500	9	0.1070E+01	0.3762E-01	0.1939E+00	0.1888E+02
1.500	0.000	11.500	10	0.1087E+01	0.4331E-01	0.2081E+00	0.2026E+02
3.500	0.000	11.500	1	0.1042E+01	0.1785E-01	0.1336E+00	0.1301E+02
3.500	0.000	11.500	2	0.1040E+01	0.1879E-01	0.1371E+00	0.1335E+02
3.500	0.000	11.500	3	0.1046E+01	0.1724E-01	0.1313E+00	0.1279E+02
3.500	0.000	11.500	4	0.1041E+01	0.1891E-01	0.1375E+00	0.1339E+02
3.500	0.000	11.500	5	0.1038E+01	0.1959E-01	0.1400E+00	0.1363E+02
3.500	0.000	11.500	6	0.1040E+01	0.2063E-01	0.1436E+00	0.1399E+02
3.500	0.000	11.500	7	0.1043E+01	0.2053E-01	0.1433E+00	0.1395E+02
3.500	0.000	11.500	8	0.1046E+01	0.1854E-01	0.1362E+00	0.1326E+02
3.500	0.000	11.500	9	0.1043E+01	0.1751E-01	0.1323E+00	0.1289E+02
3.500	0.000	11.500	10	0.1044E+01	0.2040E-01	0.1428E+00	0.1391E+02
5.500	0.000	11.500	1	0.1016E+01	0.2022E-01	0.1422E+00	0.1385E+02
5.500	0.000	11.500	2	0.1020E+01	0.1966E-01	0.1402E+00	0.1365E+02
5.500	0.000	11.500	3	0.1014E+01	0.1959E-01	0.1400E+00	0.1363E+02
5.500	0.000	11.500	4	0.1016E+01	0.2161E-01	0.1470E+00	0.1432E+02
5.500	0.000	11.500	5	0.1015E+01	0.2029E-01	0.1424E+00	0.1387E+02
5.500	0.000	11.500	6	0.1021E+01	0.1827E-01	0.1352E+00	0.1316E+02
5.500	0.000	11.500	7	0.1008E+01	0.1824E-01	0.1351E+00	0.1315E+02
5.500	0.000	11.500	8	0.1012E+01	0.1880E-01	0.1371E+00	0.1335E+02
5.500	0.000	11.500	9	0.1014E+01	0.2126E-01	0.1458E+00	0.1420E+02
5.500	0.000	11.500	10	0.1008E+01	0.2031E-01	0.1425E+00	0.1388E+02
7.500	0.000	11.500	1	0.1037E+01	0.1316E-01	0.1147E+00	0.1117E+02
7.500	0.000	11.500	2	0.1037E+01	0.1281E-01	0.1132E+00	0.1102E+02
7.500	0.000	11.500	3	0.1041E+01	0.1455E-01	0.1206E+00	0.1174E+02
7.500	0.000	11.500	4	0.1038E+01	0.1404E-01	0.1185E+00	0.1154E+02
7.500	0.000	11.500	5	0.1048E+01	0.1686E-01	0.1299E+00	0.1264E+02
7.500	0.000	11.500	6	0.1035E+01	0.1473E-01	0.1214E+00	0.1182E+02
7.500	0.000	11.500	7	0.1038E+01	0.1468E-01	0.1211E+00	0.1180E+02
7.500	0.000	11.500	8	0.1032E+01	0.1331E-01	0.1153E+00	0.1123E+02
7.500	0.000	11.500	9	0.1037E+01	0.1167E-01	0.1080E+00	0.1052E+02
7.500	0.000	11.500	10	0.1035E+01	0.1194E-01	0.1092E+00	0.1064E+02

Table 1: Sample data output from automatic data acquisition system.

APPENDIX 2

A COMPARISON OF HYBRID AND QUADRATIC-UPSTREAM DIFFERENCING IN HIGH REYNOLDS NUMBER ELLIPTIC FLOWS

by

T. Han[1], J.A.C. Humphrey[2] and B.E. Launder[3]

University of California

Report No. FM-81-1

Submitted to

Computer Methods in Applied Mechanics and Engineering

January 1981

1. Associate Research Engineer

2. Assistant Professor

   Department of Mechanical Engineering,
   University of California, Berkeley.

3. Professor

   Department of Mechanical Engineering
   University of Manchester Institute of Science and Technology,
   Manchester, England.

ABSTRACT

Numerical computations have been performed of various two-dimensional, elliptic flows at high Reynolds number with a view to assessing the relative merits of the widely used hybrid (i.e., upwind/central) interpolation and the recently proposed quadratic-upstream interpolation of Leonard, known as QUICK. The latter scheme possesses less intrinsic stability than hybrid differencing. By selectively evaluating some of the convective elements at a previous iteration level, however, satisfactorily rapid convergence has been obtained. It is concluded from the flows tested that the extra computational effort per node required for QUICK over the hybrid difference scheme is more than repaid by the greater numerical accuracy that results.

1. INTRODUCTION

The problem of numerical or "false" diffusion in elliptic flows [1] plagues the computational fluid mechanicist who requires accuracy from a prediction procedure at a reasonable cost. The situation is usually serious even in two-dimensional flows (where uneconomically fine grids are often required) while it becomes grave in three-dimensional flows with strong gradients of the dependent variables (velocity, pressure, temperature, turbulent kinetic energy, etc.). Numerical diffusion also causes difficulties for the turbulence modeler, who needs to eliminate from the computations any aberrations due to the finite-difference practices in order that his solutions reflect purely the outcome of the physical model embodied in the prediction procedure.

In two recent publications, Leonard [2,3] has reassessed the problem of numerical diffusion in convection dominated flows. In reviewing the characteristics of the more commonly used treatments, he shows [3] how central differencing may lead to unphysical oscillatory behavior in an implicit scheme or to non-convergence in an explicit computation approach in regions of the flow where convection dominates diffusion ($Pe > 2$). He also shows [3] that while upstream differencing of convective terms leads to a highly stable discretization, this stability is achieved at the expense of introducing truncation error or numerical diffusion arising from streamline-to-grid skewness, defects which may seriously impair the accuracy of the computations. If the numerical diffusion coefficient (Γ_{num}) is to be made insignificant in comparison with the physical diffusion coefficient, the mesh Peclet number, $U\Delta x/\Gamma_{num}$ must be less than 2. While grid refinement can, in principle, alleviate the problems associated with upstream differencing, the degree of refinement needed to eliminate false diffusion is often impractical. This is

especially the case in problems of engineering interest, where although the effective turbulent diffusivity may be several orders of magnitude larger than the molecular value, the flow may be three-dimensional, the boundary conditions or flow may be unsteady and the field variables may display strong non-linear variations. Leonard [2,3] in fact proposed an alternative discretization of the convective transport terms which, he claimed, while greatly reducing the numerical diffusion created by an upwind treatment, avoided the problems of instabilities found with central differencing. The approach, which Leonard, with a rare mastery of the acronym [2], styled the QUICK algorithm* employs a three-point upstream-weighted quadratic interpolation. References [2] and [3] give several examples which demonstrate the improvements in accuracy that result from the scheme. A very recent paper by Leschziner [4] provides supporting comparisons of the advantages of both QUICK and skewed-upwind differencing [5] over the hybrid treatment.

Although these signs were encouraging, it must be said that none of the reported tests have been numerically very challenging: in every case the equations were linear, the most complicated being the solution of the thermal field in a cavity with prescribed velocity field. The question of whether the QUICK algorithm would be (or could be made) sufficiently stable to justify its use in more realistic cases, where the flow field was highly non-linear and (especially in the case of turbulent flow) the equations intricately coupled was thus open to question. It is this topic that the present contribution

---

*Quadratic upstream interpolation for convective kinematics.

addresses. The following section presents the interpolation schemes used in this comparative study while Section 3 discusses the outcome of tests for the test flows examined, including cases of both laminar and turbulent flow. The paper closes with some related conclusions and recommendations.

After the initial version of this paper was completed, a manuscript Leschziner and Rodi [6] reporting a study of recirculating jet flows came to our attention. The results appearing in that paper relating to the merits of quadratic differencing are broadly in accord with those described hereunder.

2. NUMERICAL PROCEDURE

2.1 General Remarks

The flow calculation procedure used as the basic vehicle for this study is the TEACH-2E program of Gosman and Pun [7]. Velocity and pressure are solved directly as primitive variables on a staggered grid using the integrated control volume approach. The procedure has been described in detail in various references; see for example Patankar [8]. It incorporates the SIMPLE solution algorithm of Patankar and Spalding [9] whereby, for a fixed pressure field, a set of difference equations for the x and y velocity components are solved line-by-line. After completing a sweep of the entire solution domain, adjustments are made to the pressure field to ensure that continuity is satisfied along every line of cells. Such adjustments destroy the compliance of the velocity and pressure fields with the momentum equations and so further iterations are needed until the momentum and continuity equations are simultaneously satisfied to the required degree of accuracy. For turbulent flows the standard energy-dissipation rate eddy viscosity model is employed (see, for example, Launder and Spalding [10]) and the kinetic energy and dissipation equations are solved simultaneously with the mean velocity field.

The two momentum equations and the equations expressing the transport of turbulent kinetic energy, k, and its dissipation rate, ε, may be expressed in the following form:

$$\frac{\partial}{\partial x}(\rho u \phi) + \frac{\partial}{\partial y}(\rho v \phi) = \frac{\partial}{\partial x}\left(\Gamma \frac{\partial \phi}{\partial x}\right) + \frac{\partial}{\partial y}\left(\Gamma \frac{\partial \phi}{\partial y}\right) + S_0 \qquad (1)$$

where ϕ is the particular variable of interest (u, v, k, or ε), Γ is the exchange coefficient and S_0 encompasses all remaining terms and is therefore

referred to as a "source" term. In the laminar flow case (ϕ = u and v) Γ is simply the laminar viscosity, μ, and S_0 contains only the pressure gradient term. Each equation of type (1) corresponding to the different variables is converted to finite-difference form by integrating over a control volume surrounding each node. Both the discretization schemes for convective transport whose performances we compare below, have been used in conjunction with the usual central-difference approximation of the diffusion terms

$$\left(\frac{\partial^2\phi}{\partial x^2}\right)_i = \frac{\phi_{i+1} - 2\phi_i + \phi_{i-1}}{\Delta x^2} + \left[\frac{1}{12}\,\phi_i^{iv}\,\Delta x^2 + \ldots\right] \tag{2}$$

2.2 The HYBRID Scheme

In common with many other programs, TEACH-2E employs basically an upwind treatment in representing the convective terms of (1). As a minor improvement, however, central differencing is used when the local cell Reynolds number is less than 2. This hybrid scheme (henceforth called HYBRID) proposed by Spalding [11] may be stated:

$$\text{if } R_\Delta < 2;\quad u\frac{\partial\phi}{\partial x} = u\left[\frac{\phi_{i+1} - \phi_{i-1}}{2\Delta x} - \frac{1}{6}\,\phi_i'''\,\Delta x^2 + \ldots\right] \tag{3}$$

$$\text{if } R_\Delta > 2 \text{ and } u > 0;\quad u\frac{\partial\phi}{\partial x} = u\left[\frac{\phi_i - \phi_{i-1}}{\Delta x} + \frac{1}{2}\,\phi_i''\,\Delta x + \ldots\right] \tag{4}$$

$$\text{if } R_\Delta > 2 \text{ and } u < 0;\quad u\frac{\partial\phi}{\partial x} = u\left[\frac{\phi_{i+1} - \phi_i}{\Delta x} - \frac{1}{2}\,\phi_i''\,\Delta x + \ldots\right] \tag{5}$$

It is clear from equations (4) and (5) that although the truncation error is formally proportional to Δx, the actual size of the error depends on the second

spatial derivative of ϕ throughout the computational domain. The upstream difference scheme will therefore be free of first-order truncation error (which is the main source of numerical diffusion) only if the function ϕ is linear in x; any function which has a local extremum must involve a non-zero first-order truncation error. Leonard [2] argues that, for convection dominated flows, HYBRID is only marginally superior to pure upwind differencing and its use places very severe limitations on the coarseness of grid that will allow useful numerical accuracy to be obtained.

2.3 The QUICK Scheme

In following the control-volume approach to derive a set of finite-difference equations, the main concern is to estimate accurate values of the dependent variables at the surfaces of the control volume while avoiding the instability associated with high convection rates. For central differencing, the estimate is based on a linear interpolation which gives a second-order truncation error; but the scheme becomes *unstable* for $R_\Delta > 2$. A parabolic polynomial interpolation, which simultaneously possesses higher accuracy and stable convective sensitivity, provides an alternative approach. The control-volume surface values are obtained by fitting a parabola to the values of ϕ at three consecutive nodal positions, the two nodes located on either side of the surface in question plus the next node on the upstream side. Examples of quadratic interpolation expressions for a uniform grid spacing are given by the following expressions, (see Fig. 1):

$$\text{if } u_e > 0;\ \phi_e = \frac{1}{2}(\phi_i + \phi_{i+1}) - \frac{1}{8}(\phi_{i-1} + \phi_{i+1} - 2\phi_i) \tag{6}$$

$$\text{if } u_e < 0;\ \phi_e = \frac{1}{2}(\phi_i + \phi_{i+1}) - \frac{1}{8}(\phi_i + \phi_{i+2} - 2\phi_{i+1}) \tag{7}$$

These expressions may be interpreted as linear interpolations for ϕ_e corrected by the inclusion of terms proportional to the respective upstream-weighted curvatures. If the latter terms in (6) and (7) are omitted, the central-difference form is recovered. Initially, forms (6) and (7) were incorporated into TEACH by treating the central-difference part as the true convective term and accommodating the curvature correction as an explicit source term using the current value of the ϕ's in question. This proved to be unstable for all cases examined through loss of diagonal dominance. False transient techniques were evolved that did succeed in procuring convergence albeit rather slowly (roughly 2½ times as many iterations as for HYBRID). Subsequently, several alternative decompositions of the difference formulae were tested and, of these, the following alternative groupings secured convergence for laminar flows without the addition of false-transient terms:

$$\left.\begin{aligned} &\text{if } u_e > 0 ; \quad \phi_e = \tfrac{1}{8}\left(-\phi_{i-1} + 6\phi_i + 3\phi_{i+1}\right) \\ &\text{if } u_e < 0 ; \quad \phi_e = \tfrac{1}{8}\left(3\phi_i + 6\phi_{i+1}\right) \underbrace{- \tfrac{1}{8}\phi_{i+2}}_{\text{source}} \end{aligned}\right\} \tag{8}$$

$$\left.\begin{aligned} &\text{if } u_e > 0 ; \quad \phi_e = \tfrac{1}{8}\left(6\phi_i + 4\phi_{i+1}\right) \underbrace{- \tfrac{1}{8}\left(\phi_{i-1} + \phi_{i+1}\right)}_{\text{source}} \\ &\text{if } u_e < 0 ; \quad \phi_e = \tfrac{1}{8}\left(3\phi_i + 4\phi_{i+1}\right) \underbrace{- \tfrac{1}{8}\left(\phi_{i+2} - 2\phi_{i+1}\right)}_{\text{source}} \end{aligned}\right\} \tag{9}$$

Equations (8) generally led to faster convergence (about 35% more iterations than HYBRID) but occasionally the scheme diverged; we would therefore recommend equations (9) (requiring about 50% more iterations than HYBRID) as the safer. In both cases the source parts are all evaluated with values determined at

the *previous* level of iteration. The latter is an important point to observe since we found that if, instead, we used "latest available" values of ϕ convergence was either destroyed or at least greatly impaired.

In calculations for turbulent flow, the strong coupling between the turbulent and mean-flow fields has meant that we have had to use in addition a pseudo-transient term that went to zero as a converged solution was approached. For this case the general form of the difference equation for ϕ at the center P of a cell is given by

$$\phi_P = \frac{\Sigma A_i \phi_i + S_o + \frac{\Delta m_P}{\Delta t} \phi_P^*}{\Sigma A_i + \frac{\Delta m_P}{\Delta t}} \tag{10}$$

Convective and diffusive effects, embodied in the A_i coefficients, are summed over the nodes neighboring with P; S_o is a possible source term. The false-transient term $\frac{\Delta m_P}{\Delta t} \phi_P^*$ (where $\Delta m = \rho \Delta V$ represents the mass of the cell at P, and * denotes the value of ϕ_P at the previous iteration) does not affect the final solution although it significantly affects the rate of convergence. No general rule has been obtained for finding the optimum value of Δt in the false transient term which must be determined from numerical experimentation.

3. TEST CASES, RESULTS AND DISCUSSION

3.1 Axisymmetric Irrotational Stagnation Flow

To obtain some understanding of the behavior of the differencing schemes, the axisymmetric impingement of a semi-infinite extent of an ideal irrotational fluid on a plane wall was examined. The enforced turning of the streamlines from the direction normal to the wall to that parallel to it necessitates that, with a rectangular grid, the flow lines cut diagonally across the grid. Although not shown here, the computed velocity fields for HYBRID* and QUICK were in excellent agreement with the exact solution. However, a significant difference in the pressure field was observed as shown in Fig. 2. With a relatively coarse 12 x 12 uniform grid, the pressure distribution of QUICK along $r/L = 0.05$ shows very good agreement with the elliptic surface of the exact solution. The result for HYBRID differencing is far less accurate with the same grid refinement. Indeed, even when the mesh in this case is refined to 22 x 22, differences shown for the HYBRID treatment are an order of magnitude larger than for QUICK. We note that while the velocity field is linear in this flow (which is why HYBRID differencing leads to such accurate results for the velocity field), the corresponding pressure distribution is quadratic in velocity and therefore amplifies the first order truncation error of the upstream differencing approach.

*Since the viscosity is zero in this problem, the HYBRID treatment is identical to upwind differencing.

3.2 Laminar Flow Cases

Two viscous recirculating flows, the wall-driven cavity and the flow downstream from a sudden pipe expansion, were selected as a second class of test cases.

Because of its geometric simplicity yet strongly elliptic character, the wall driven cavity has been widely used for examining numerical discretizations of the Navier-Stokes equations. Many of the calculated results available in the literature show only streamline contour plots without specific velocity distributions. This has precluded carrying out direct and detailed comparisons with various studies of relevance to this work. However, Burggraf [13] has performed an excellent numerical study for the case of a square cavity, using a sequence of successively refined grids for a range of progressively increasing Reynolds numbers. He employed central differences for the non-linear convective terms in the transport equations.

Computations for HYBRID, central and QUICK schemes were carried out with the TEACH code by simply replacing the treatment of non-linear convection terms, respectively.* The computed results of these three numerical schemes using a uniform grid were compared directly with velocity distributions obtained by Burggraf for Reynolds numbers of 100 and 400 based on cavity width and lid velocity. A comparison among the schemes is also provided at a Reynolds number (R_e) of 1000.

---

*A false transient treatment was required to stabilize the central difference solution.

At R_e = 100, shown in Fig. 3, excellent agreement is observed among the three schemes for the variation of horizontal velocity (u) along the central vertical line. At higher Reynolds numbers the approximations adopted for convection have significantly more influence on the accuracy of the final solution. If we take Burggraf's results as correct, at R_e = 400, shown in Fig. 4, the HYBRID scheme is less accurate than the QUICK or central difference scheme.

The velocity profile based on QUICK with a moderate number of grid nodes (22 x 22) shows almost exact agreement with Burggraf's (40 x 40) grid calculations. The present calculations using central differencing scheme on a 22 x 22 grid show close but not as good agreement with Burggraf's result, while the HYBRID treatment leads to a 10% under-estimate of the flow rate of recirculating fluid.

At a Reynolds number of 1000, velocity profiles given in Fig. 5, calculated using the central and QUICK difference schemes, show a fairly close correspondence. Although one cannot write with certainty, it would appear from the results at R_e = 400 that the results given by QUICK would be the more accurate. The HYBRID calculations show a significantly different behavior, the recirculating mass flow rate now being fully 25% less than for QUICK.

Figure 6 compares velocity profiles obtained with the HYBRID and QUICK schemes for three different grid refinements. The result for QUICK with 22 x 22 grid is probably accurate enough to be regarded as a grid-independent solution even at this high Reynolds number. By contrast, the HYBRID scheme result for a 30 x 30 grid is fairly similar to the velocity distribution generated by QUICK with an 8 x 8 grid (which is omitted for clarity). Evidently, substantial savings in computing time and storage can be made with

quadratic upstream interpolation, especially in three-dimensional flows.

As a footnote to the explorations of laminar flow in a driven cavity, we remark that at $R_e = 10^5$ none of the methods we have tried for incorporating QUICK produced a converged solution. The result is neither particularly surprising nor alarming since it is unlikely that a stable, steady-flow solution to the Navier-Stokes equations exist at such a high Reynolds number. In contrast, HYBRID leads unerringly to a converged result.

The flow downstream of a sudden pipe expansion also provides a relatively simple elliptic flow. In contrast to the driven cavity example, however, the shape of the recirculating region is not directly enforced by the boundary conditions. For numerical accuracy the best distribution of nodes for this problem would be non-uniform with a concentration in the thin shear layer that springs from the expansion corner. The present tests were, however, made with a uniform radial distribution of nodes as the results are principally for comparative purposes. Uniform inlet axial velocity was prescribed, no-slip conditions on the walls and zero streamwise gradient of u and v at the exit. Figure 7 shows axial velocity profiles at several streamwise positions for a Reynolds number based on inlet velocity and upstream diameter of 500 and a diametral expansion ratio of 2:1. In contrast to the cavity flow, there is now virtual agreement between the two results. The reason for this is that the recirculation region is now highly elongated, reattachment occurring approximately 19 step heights downstream. The streamlines are thus nearly parallel to the grid lines and the false diffusivity, which is roughtly equal to $0.3\ [(u^2 + v^2)\ \Delta x \Delta y]^{\frac{1}{2}} \sin 2\theta$ is typically an order of magnitude less than ν because θ, the local angle between the grid line and the velocity vector is so small. Only in parts of the recirculation zone and in the immediate vicinity of the reattachment point do the streamlines cut at a substantial

angle with the grid and there velocities are low. The results for a Reynolds number of 1000 again show little difference between the two treatments because the angle between the grid and the streamlines becomes even smaller.

3.3 Turbulent Flow

In turbulent flows bounded by walls, there is a very marked variation of effective turbulent viscosity over the flow field. Moreover, the turbulent viscosity is popularly obtained by a transport model in which, typically, the local values of two scalar properties of turbulence are obtained from transport equations solved simultaneously with those for the mean flow. These turbulent transport equations contain major source and sink terms which provide an intricate coupling with the mean motion that has no counterpart in laminar flow. For these reasons one cannot reliably draw conclusions about the general efficacy of a particular discretization scheme from laminar flow tests alone. Both the square, wall-driven cavity and the pipe expansion have been examined for turbulent flow conditions employing the standard high Reynolds number form of the $k \sim \varepsilon$ viscosity model, [10]. For each case converged results were much harder to achieve than for the corresponding laminar flow. The practice we have adopted is to use the HYBRID solution as the initial field for beginning the iteration with QUICK. Moreover, the iterations proceed using false-transient stabilization with different effective time steps in different regions of the flow domain. With these measures, converged solutions were typically obtained in about 250 iterations. As with laminar flow, the numerical results for the flow downstream of a pipe expansion display only minor differences between the two convective approximations and are not included here; those for the square cavity are much more pronounced and are discussed below.

Besides pure HYBRID and QUICK solutions, a third practice, employed by Leschziner and Rodi [6], has been tested, in which the QUICK approximation is applied to the x- and y- momentum equations while the HYBRID scheme is used for the transported turbulence variables, k and ε. The reason given by Leschziner and Rodi for this mixed treatment was that the two turbulence equations were so dominated by source terms that the values generated for k and ε would be virtually immune to the effects of false diffusion. Whether or not they had tried an orthodox QUICK treatment in the course of their work is not stated. Mean velocity distributions along a central vertical line (running from the floor to the roof of the cavity) are shown in Fig. 8 for a Reynolds number of 10^5. Because the grid is fairly refined (40 × 40) false diffusion is small in all cases and differences between the mean velocity profiles corresponding to the different convective treatments are minor. However, the coarse grid (22 × 22) calculations of mean velocity shown in Figure 9 display significant differences among the various convective treatments. Figure 11, to be discussed in detail below, shows that in going from a refined to a coarse grid the level of turbulent viscosity calculated using the QUICK approach does not change much. The change is large, however, for the HYBRID and the mixed convective treatments. Thus turbulent viscosity is considerably underestimated on a 22 × 22 grid by the latter two treatments. It is only the fortuitous compensation by false-diffusion in the HYBRID scheme which leads to the incorrect impression that the HYBRID scheme velocity profile calculations are fairly insensitive to changes in grid refinement. Note that because the mixed convective treatment is less prone to numerical diffusion (and hence its compensating effects) than the pure HYBRID approach, it is the *most* sensitive to changes in grid refinement.

The distorting effects of false diffusion are more vividly displayed in Figures 10-a and b where vector velocity plots of wall driven cavity

flow corresponding to the HYBRID and QUICK treatments are contrasted. The calculations were performed on a 40 × 40 grid for a Re = 10^5. Clearly shown for the QUICK treatment are three recirculation zones, in the top two corners and the bottom right hand corner of the cavity flow respectively, which are not resolved by the HYBRID treatment.

The effect of grid refinement on the calculated distribution of turbulent viscosity is shown in Fig. 11. Here it should be noted that with the model adopted, the level of turbulent viscosity is given by 0.09 k^2/ε. In the central region of the cavity the levels of k and ε are very dependent upon diffusion since the generation terms in their respective conservation equations vanish and the sink terms remain non-zero. The calculated level of ν_t is thus particularly sensitive to *numerical* diffusion. In fact, a refinement of the grid from (22 x 22) to (40 x 40) produces roughly a *three-fold* increase in turbulent viscosity in the central region of the cavity for both the HYBRID and the mixed treatments. The direction of the change is easily understood. In the turbulence model, the diffusion coefficient for turbulence energy, k, is about 50% greater than that for ε; each variable, however, may be supposed to be roughly equally prone to *false* diffusion. Consequently, numerical smearing will lead to too large levels of ε and, since ε is the sink in the k equation, to too low levels of turbulence energy; through this doubled-edged effect the quantity k^2/ε turns out to be exceptionally low.

When QUICK is used for all dependent variables, the variation of ν_t in the central region arising from the same grid refinement is reduced to only 25%. It is of interest to note that for the 40 x 40 grid the calculated level of ν_t with QUICK is uniform in the central region while the other two treatments display a waviness similar to that produced by QUICK with the coarser mesh. This result leaves little doubt that among the three versions examined QUICK provides the most accurate representation of convective transport.

4. CONCLUSIONS

(i) In both laminar and turbulent flow tests Leonard's QUICK scheme has been found to give markedly superior numerical accuracy than the HYBRID treatment, a conclusion which reinforces and broadens the conclusions of Leonard [2] and Leschziner [4].

(ii) Unlike HYBRID, QUICK is not unconditionally stable. Of several alternative treatments explored for laminar flow, that given by equation (9) was found to give the most satisfactory overall convergence rates.

(iii) For turbulent flow, where there is strong non-linear coupling between the mean-flow and turbulent variables, a false transient treatment (equation (10)) had to be employed to ensure convergence.

(iv) Studies of turbulent flow in a driven cavity, suggest that, to gain the full benefits of QUICK, the solution of the turbulent variables k and ε as well as the mean velocities should incorporate a quadratic approximation of the convective terms.

Acknowledgements

The authors are grateful to the Office of Naval Research (Power Program) for supporting this work through Contract No. NOO 014-30-C-0031. Frequent and stimulating discussions with Dr. P. LeQuere, provided inputs which have been of considerable value to the study.

Authors names appear alphabetically.

REFERENCES

1. P.J. Roache, *Computational Fluid Dynamics*, Hermosa Publishers, Albuquerque, New Mexico, 1976.

2. B.P. Leonard, "A Survey of Finite Differences of Opinion on Numerical Muddling of the Incomprehensible Defective Confusion Equation", from "Finite Element Methods in Convection Dominated Flows", Applied Mechanics Division, ASME Winter Annual Meeting, New York, Dec. 1979.

3. B.P. Leonard, "A Stable and Accurate Convective Modelling Procedure Based on Quadratic Upstream Interpolation", Comp. Meths. Appl. Mech. Eng., 19, p. 59, 1979.

4. M.A. Leschziner, "Practical Evaluation of Three Finite-Difference Schemes for the Computation of Steady-State Recirculating Flows", Comp. Meths. in Appl. Mech. Eng., 1980.

5. G.D. Raithby, Comp. Meths. Appl. Mech. Eng., 9, p. 75, 1976.

6. M.A. Leschziner and W. Rodi, "Calculation of Annular and Twin Parallel Jets Using Various Discretization Schemes and Turbulence Model Variants", manuscript submitted to ASME J. Fluids Eng., 1980.

7. A.D. Gosman and W.M. Pun, Lecture notes for course entitled, "Calculation of Recirculating Flows", Imperial College HTS/74/2, 1974.

8. S.V. Patankar, "Numerical Prediction of Three-Dimensional Flows", B.E. Launder, (ed.), *Studies in Convection*, 1, p.1, Academic Press, New York, 1975.

9. S.V. Patankar and D.B. Spalding, "A Calculation Procedure for Heat, Mass and Momentum Transfer in Three-Dimensional Parabolic Flows", Int. J. Heat and Mass Transfer, 15, p. 1787, 1972.

10. B.E. Launder and D.B. Spalding, "The Numerical Computation of Turbulent Flows", Comp. Meths. Appl. Mech. Eng., 3, p. 269, 1974.

11. D.B. Spalding, "A Novel Finite Difference Formulation for Differential Expressions Involving both First and Second Derivatives", Int. J. Numerical Methods in Engineering, 4, pp. 551-559, 1972.

12. G.D. Raithby, "Skew Upstream Differencing Schemes for Problems Involving Fluid Flow", Comp. Meths. Appl. Mech. Eng., 9, p. 153, 1976.

13. O.R. Burggraf, "Analytical and Numerical Studies of the Structure of Steady Flows", J. Fluid Mech., 24, p. 113, 1966.

14. V.S. Pratap and D.B. Spalding, "Numerical Computation of the Flow in Square Ducts", Aeronaut. Q., 26, 219, 1975.

FIGURE CAPTIONS

Figure 1 Nodal configuration for the east wall boundary of a cell at i.

Figure 2 Pressure distribution in axisymmetric, inviscid stagnation flow along r/L = 0.05.

Figure 3 Velocity profiles on vertical centreline of wall-driven square cavity flow for Re = 100.

Figure 4 Velocity profiles on vertical centreline of wall-driven square cavity flow for Re = 400.

Figure 5 Velocity profiles on vertical centreline of wall-driven square cavity flow for Re = 1000.

Figure 6 Effect of grid refinement on the calculation of wall-driven square cavity flow for Re = 1000.

Figure 7 Axial velocity profiles for laminar flow downstream of a pipe expansion.

Figure 8 Mean velocity profiles for turbulent flow in a square, wall-driven cavity; calculations on a 40 × 40 grid.

Figure 9 Mean velocity profiles for turbulent flow in a square, wall-driven cavity; calculations on a 22 × 22 grid.

Figure 10 Vector velocity plots of HYBRID (A) and QUICK (B) calculations of square wall-driven cavity flow for Re = 10^5 on a 40 × 40 grid. Bottom wall drives the flow, scale is in decimeters/second.

Figure 11 Effect of grid refinement on the computed distribution of turbulent viscosity.

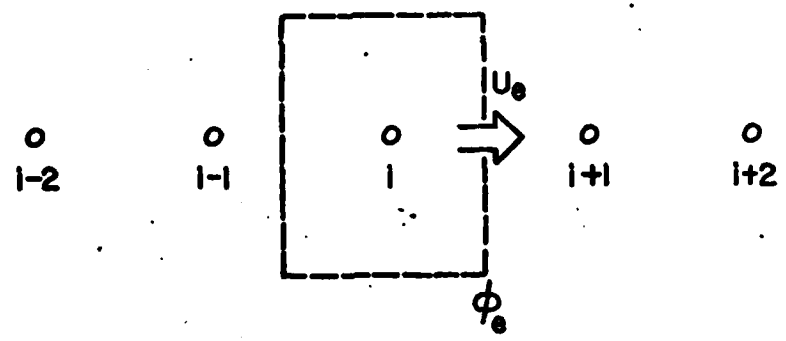

FIGURE 1

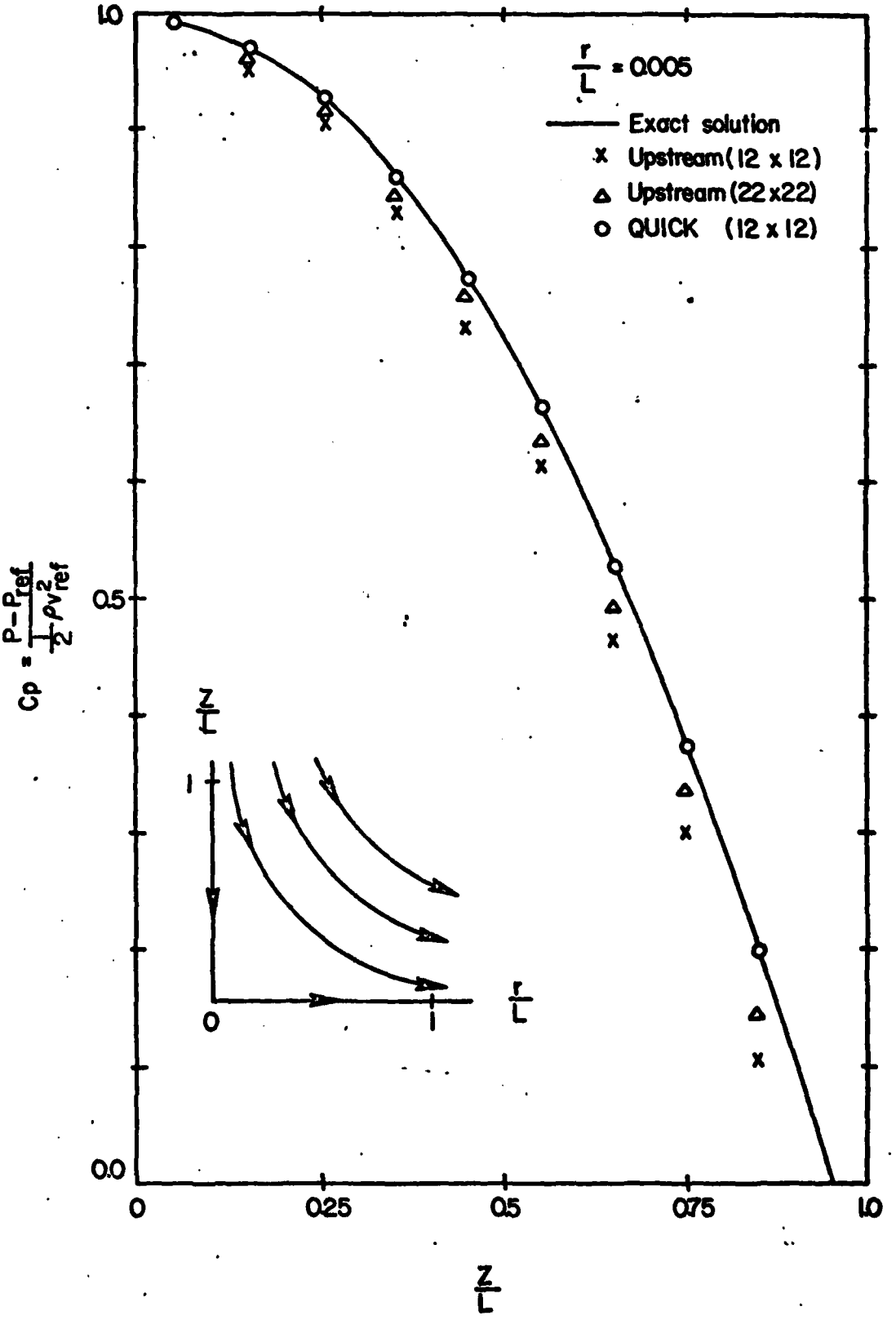
1.0
0.5
0.0
0
0.25
0.5
0.75
1.0
$\frac{r}{L}$ = 0.005
Exact solution
Upstream (12 x 12)
Upstream (22 x 22)
QUICK (12 x 12)
$C_p = \frac{P - P_{ref}}{\frac{1}{2}\rho V_{ref}^2}$
$\frac{Z}{L}$
$\frac{r}{L}$
1
0

FIGURE 2

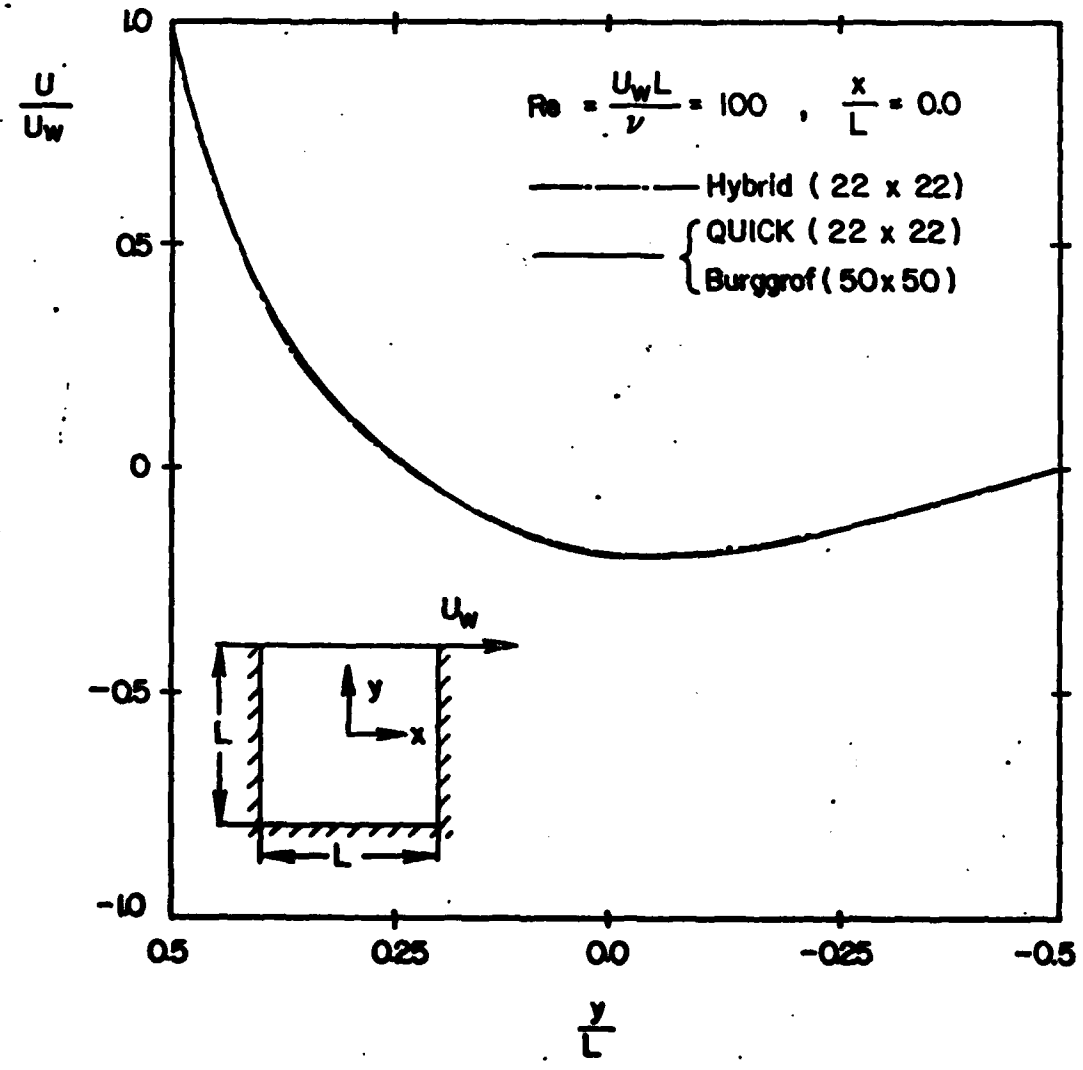
1.0
0.5
0
-0.5
-1.0
0.5
0.25
0.0
-0.25
-0.5
U/Uw
y/L
Re = UwL/ν = 100 , x/L = 0.0
Hybrid (22 x 22)
QUICK (22 x 22)
Burggrof (50x50)
Uw
y
x
L
L

FIGURE 3

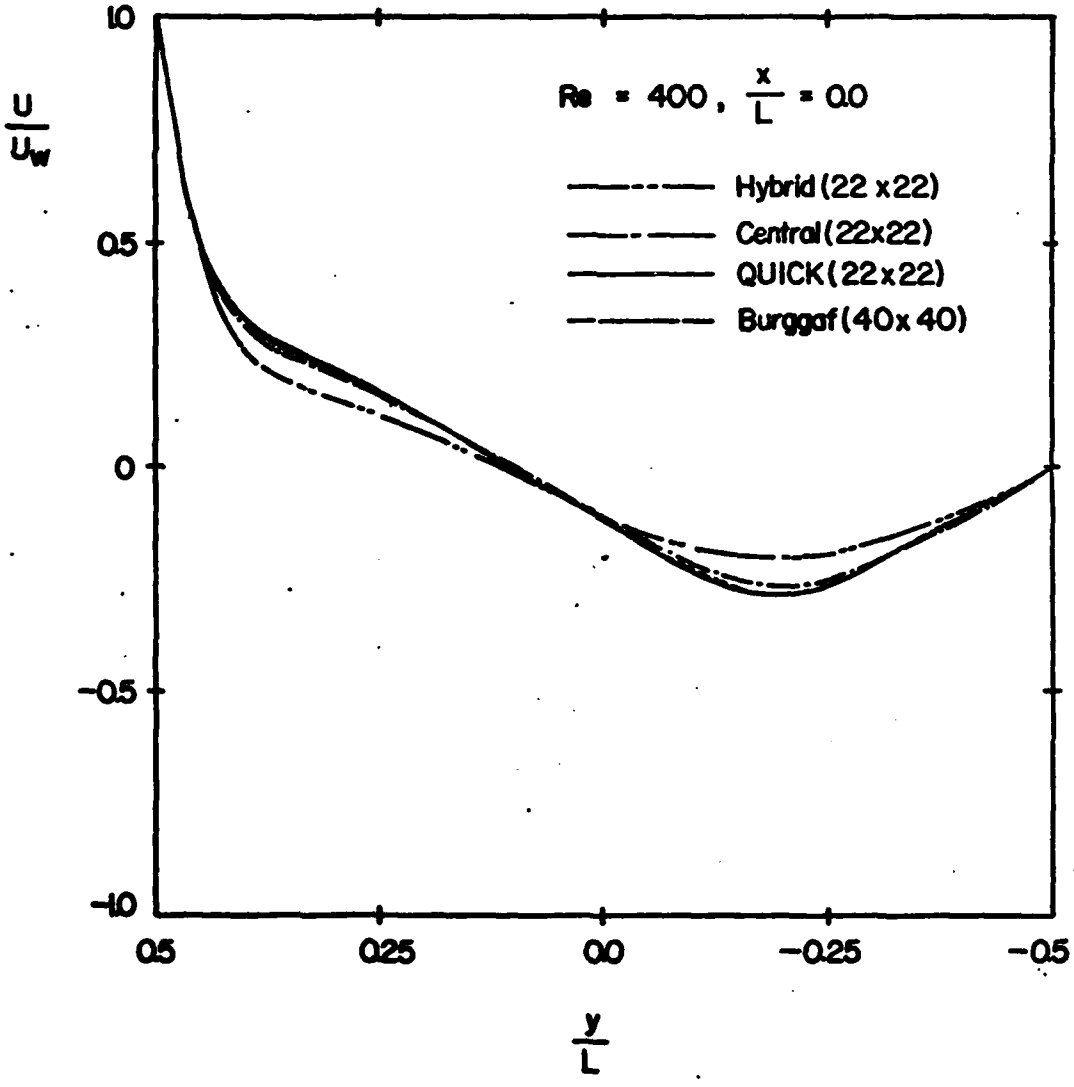
Re = 400, x/L = 0.0
Hybrid (22 x 22)
Central (22x22)
QUICK (22x22)
Burggaf (40x40)
1.0
0.5
0
-0.5
-1.0
0.5
0.25
0.0
-0.25
-0.5
U/Uw
y/L

FIGURE 4

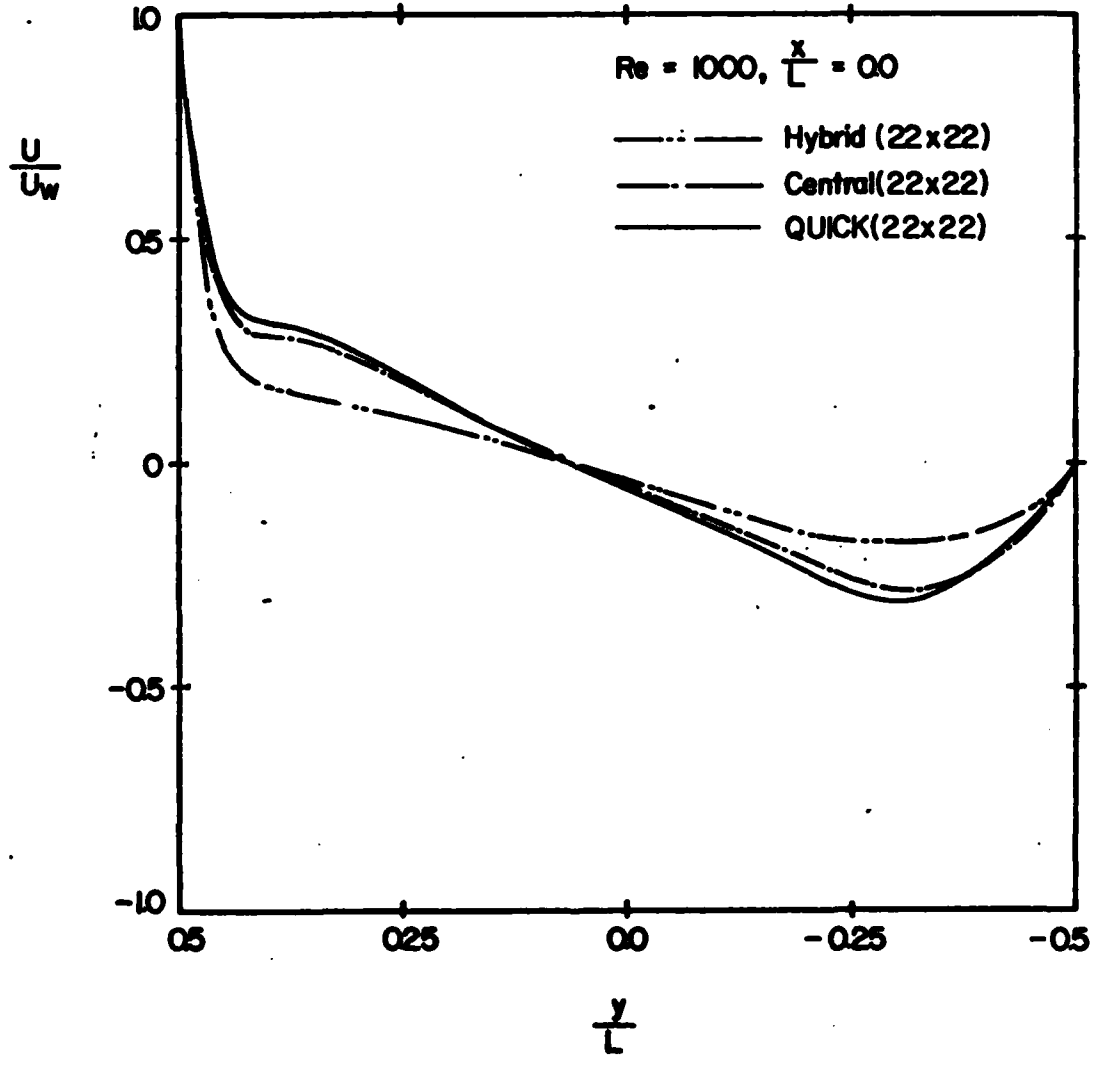
Re = 1000, $\frac{x}{L}$ = 0.0
Hybrid (22x22)
Central(22x22)
QUICK(22x22)
$\frac{U}{U_w}$
1.0
0.5
0
-0.5
-1.0
0.5
0.25
0.0
-0.25
-0.5
$\frac{y}{L}$

FIGURE 5

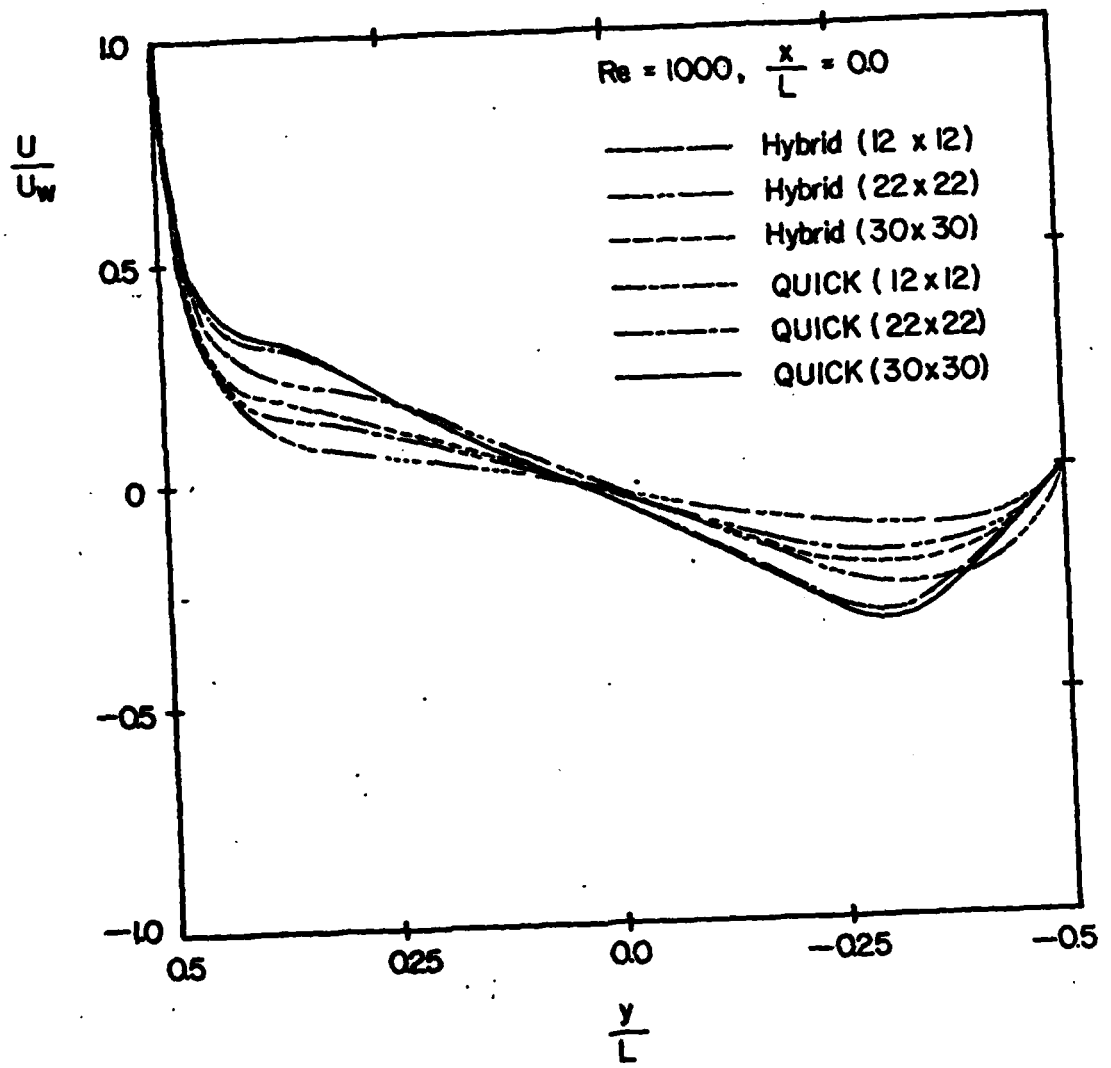
Re = 1000, x/L = 0.0
Hybrid (12 x 12)
Hybrid (22x22)
Hybrid (30x30)
QUICK (12x12)
QUICK (22x22)
QUICK (30x30)
U/Uw
y/L
1.0
0.5
0
-0.5
-1.0
0.5
0.25
0.0
-0.25
-0.5

FIGURE 6

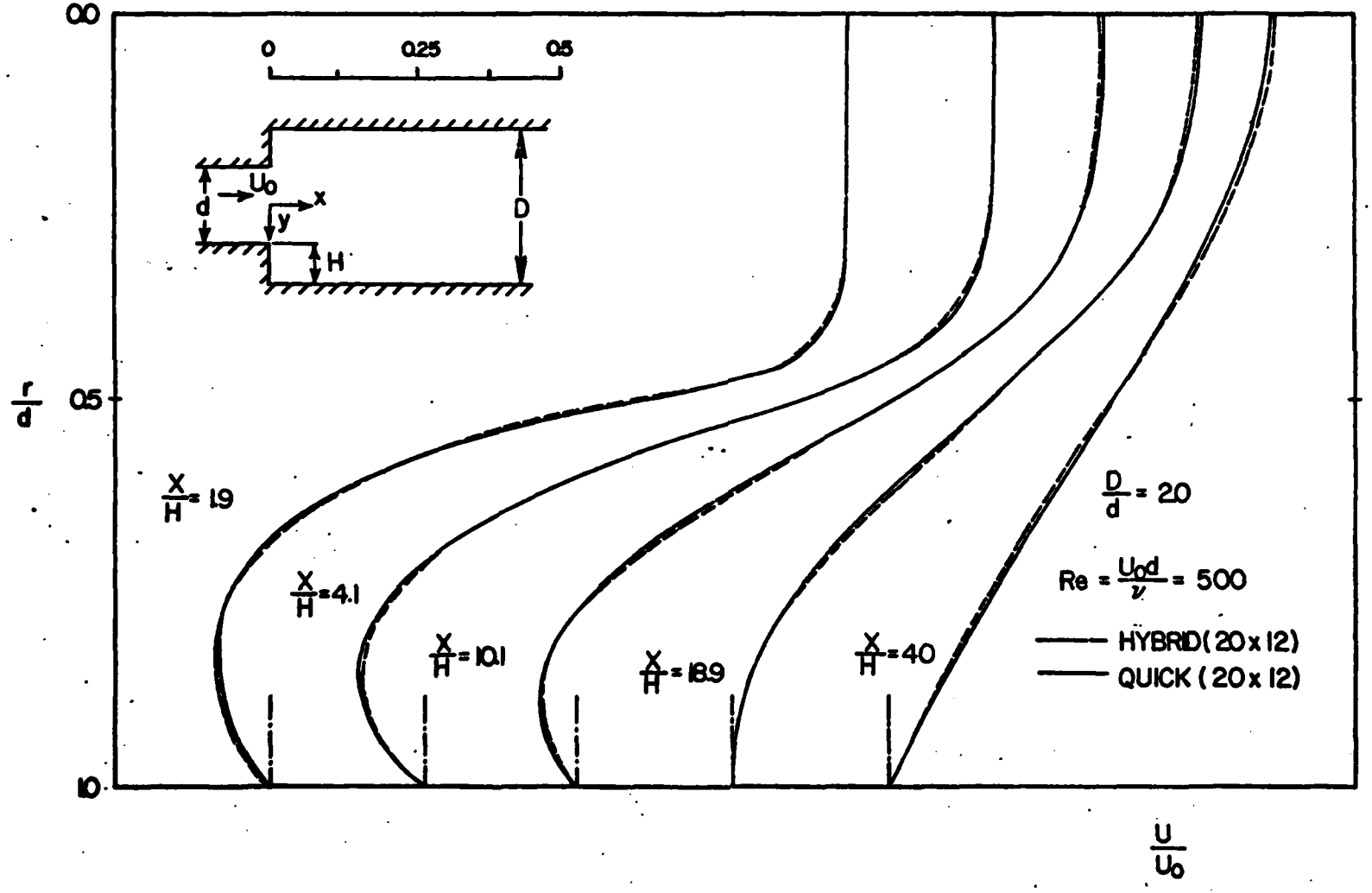
00
0
0.25
0.5
U_0
d
x
y
D
H
$\frac{r}{d}$
0.5
1.0
$\frac{X}{H}$= 1.9
$\frac{X}{H}$=4.1
$\frac{X}{H}$=10.1
$\frac{X}{H}$=18.9
$\frac{X}{H}$=40
$\frac{D}{d}$= 2.0
$Re = \frac{U_0 d}{\nu}$ = 500
HYBRID(20x12)
QUICK (20x12)
$\frac{U}{U_0}$

FIGURE 7

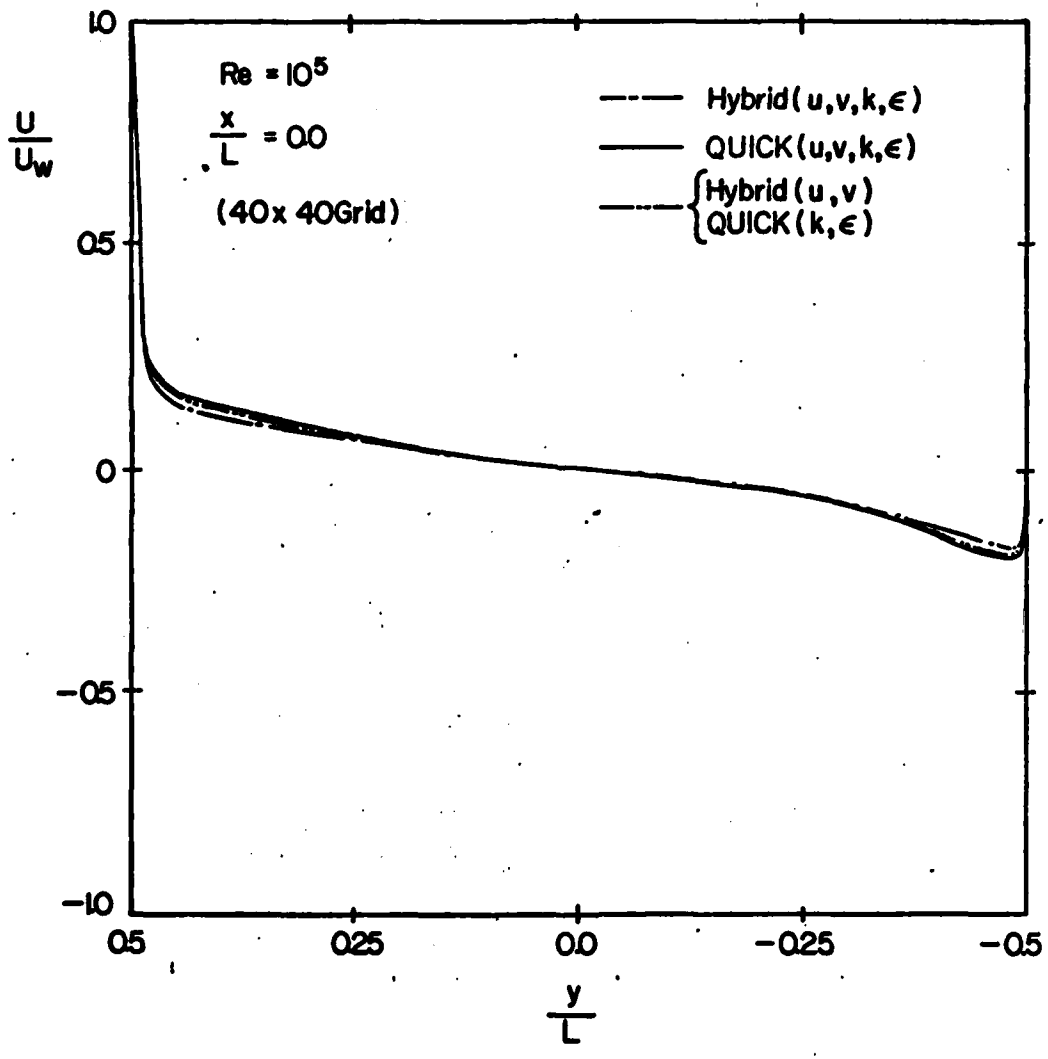
Re = 10^5
x/L = 0.0
(40 x 40 Grid)
Hybrid(u,v,k,ε)
QUICK(u,v,k,ε)
Hybrid(u,v)
QUICK(k,ε)
U/U_w
y/L
1.0
0.5
0
-0.5
-1.0
0.5
0.25
0.0
-0.25
-0.5

FIGURE 8

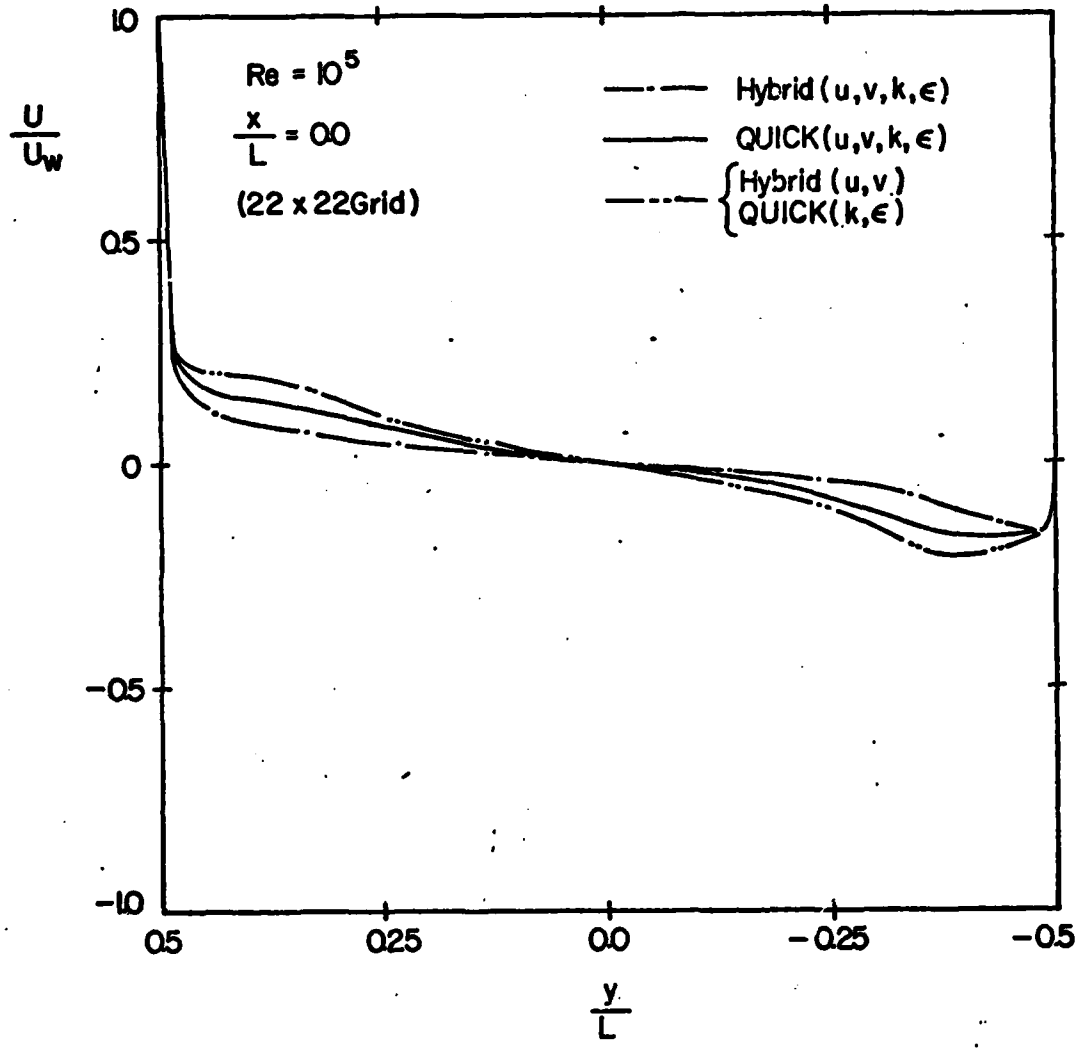
Re = 10^5
x/L = 0.0
(22 x 22 Grid)
Hybrid (u,v,k,ε)
QUICK(u,v,k,ε)
Hybrid (u,v)
QUICK(k,ε)
U/U_w
y/L
1.0
0.5
0
-0.5
-1.0
0.5
0.25
0.0
-0.25
-0.5

FIGURE 9

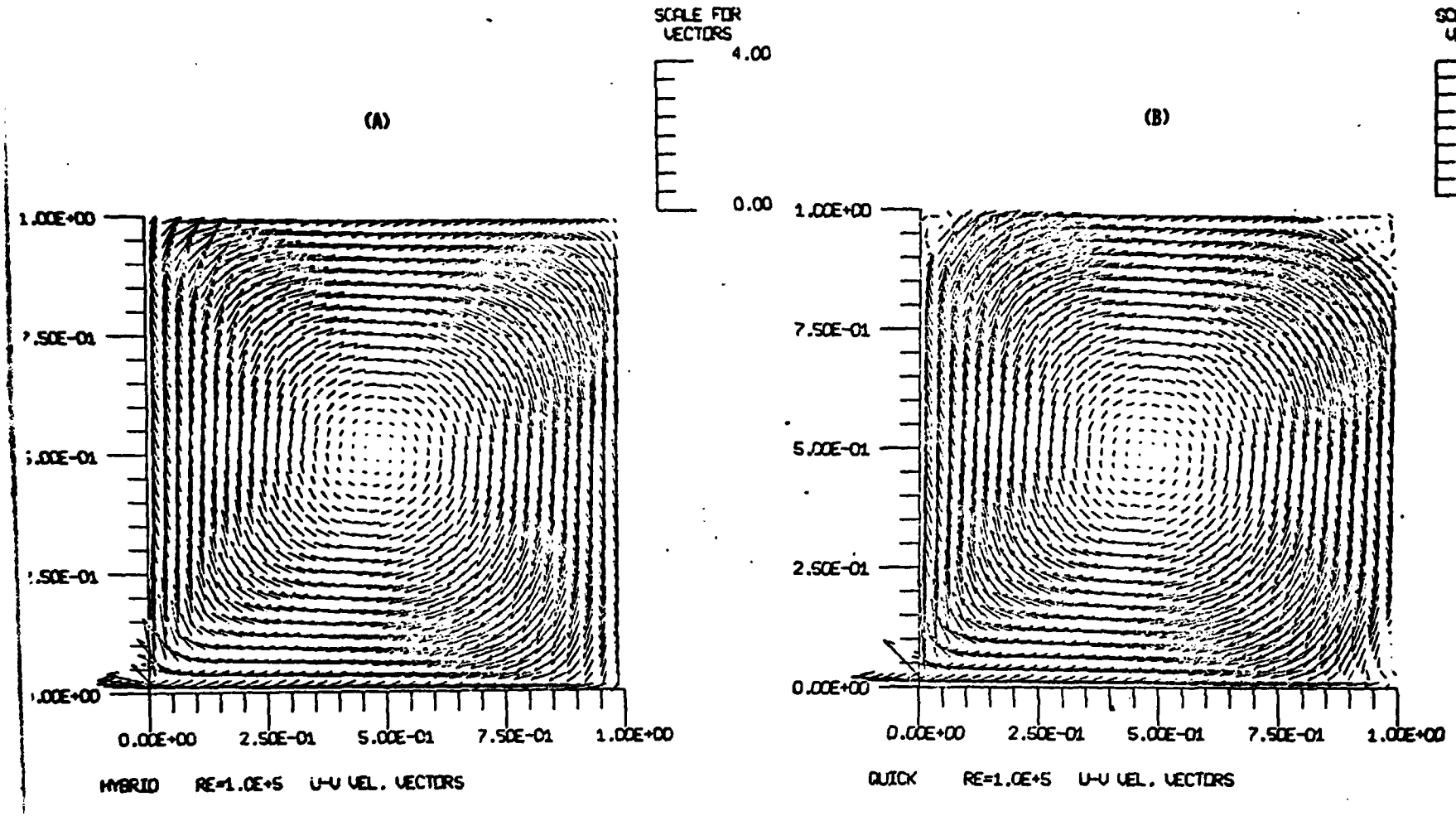
(A)
SCALE FOR VECTORS
4.00
0.00
1.00E+00
7.50E-01
5.00E-01
2.50E-01
0.00E+00
0.00E+00
2.50E-01
5.00E-01
7.50E-01
1.00E+00
HYBRID RE=1.0E+5 U-V VEL. VECTORS
(B)
SCALE FOR VECTORS
4.00
0.00
1.00E+00
7.50E-01
5.00E-01
2.50E-01
0.00E+00
0.00E+00
2.50E-01
5.00E-01
7.50E-01
1.00E+00
QUICK RE=1.0E+5 U-V VEL. VECTORS

FIGURE 10

AD-A097 461 CALIFORNIA UNIV BERKELEY DEPT OF MECHANICAL ENGINEERING F/G 20/4
TURBULENT FLOW AND HEAT TRANSFER IN PASSAGE AROUND 180 DEGREE B--ETC(U)
FEB 81 J A HUMPHREY, B E LAUNDER N00014-80-C-0031

UNCLASSIFIED NL

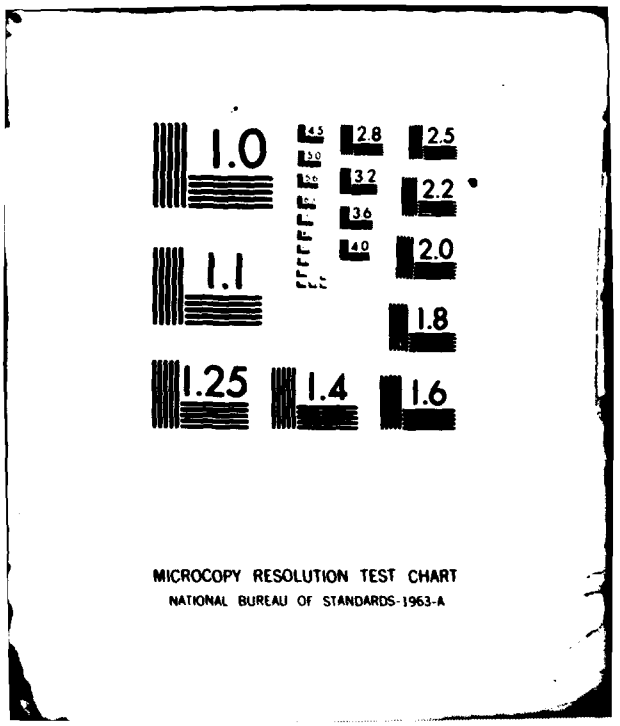
1.0
1.1
1.25
1.4
1.6
1.8
2.0
2.2
2.5
2.8
3.2
3.6
4.0
4.5
5.0
5.6
MICROCOPY RESOLUTION TEST CHART
NATIONAL BUREAU OF STANDARDS-1963-A

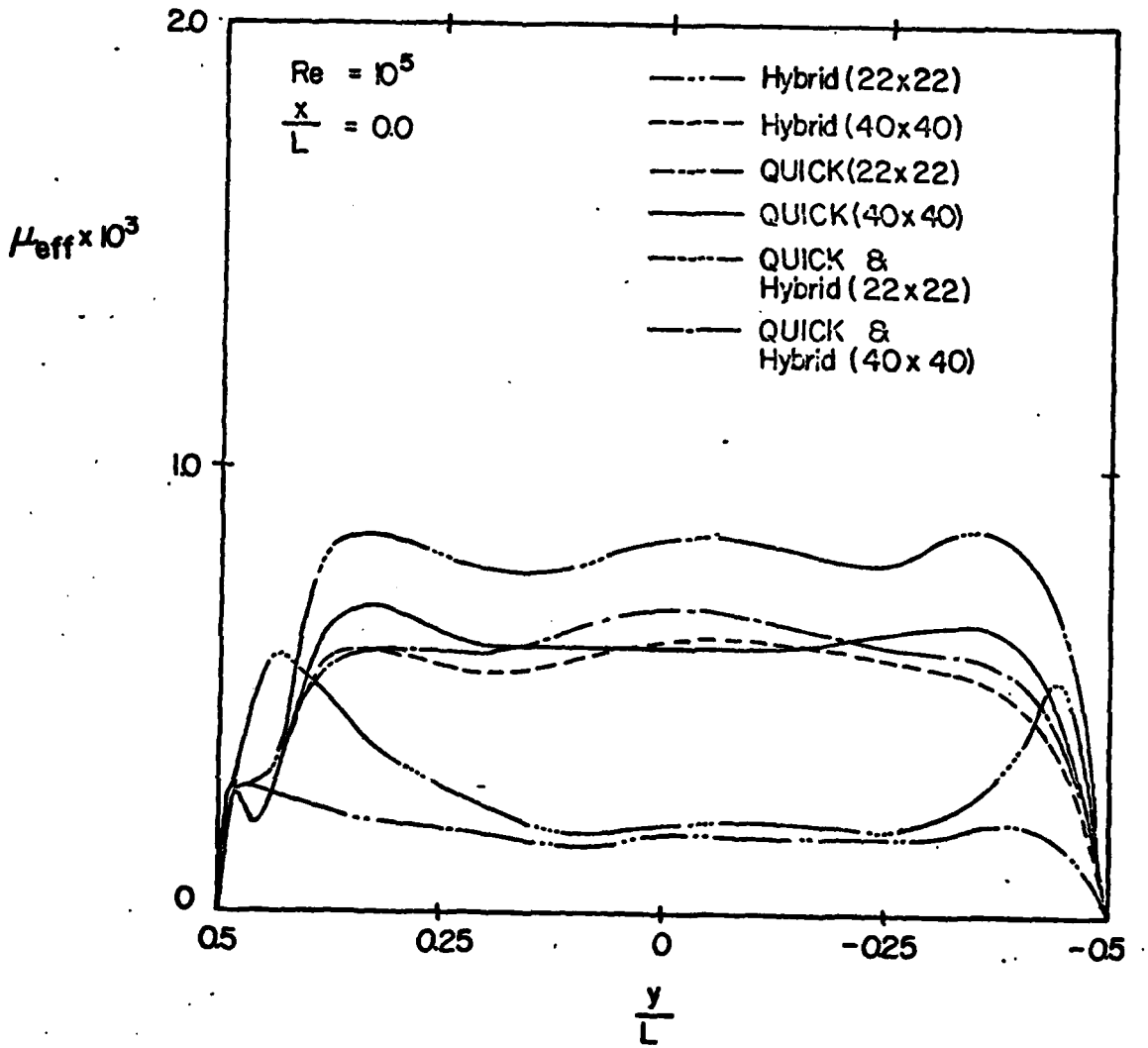
Re = 10^5
$\frac{x}{L}$ = 0.0
Hybrid (22x22)
Hybrid (40x40)
QUICK (22x22)
QUICK (40x40)
QUICK & Hybrid (22x22)
QUICK & Hybrid (40x40)
$\mu_{eff} \times 10^3$
2.0
1.0
0
0.5
0.25
0
-.025
-.05
$\frac{y}{L}$

FIGURE 11

DISTRIBUTION LIST

HEAT TRANSFER

	One copy except as noted
Mr. M. Keith Ellingsworth Power Program Office of Naval Research 800 N. Quincy Street Arlington, VA 22203	5
Defense Documentation Center Building 5, Cameron Station Alexandria, VA 22314	12
Technical Information Division Naval Research Laboratory 4555 Overlook Avenue SW Washington, DC 20375	6
Professor Paul Marto Department of Mechanical Engineering US Naval Post Graduate School Monterey, CA 93940	
Professor Bruce Rankin Naval Systems Engineering US Naval Academy Annapolis, MD 21402	
Office of Naval Research Eastern/ Central Regional Office Bldg 114, Section D 666 Summer Street Boston, Massachusetts 02210	
Office of Naval Research Branch Office 536 South Clark Street Chicago, Ill. 60605	
Office of Naval Research Western Regional Office 1030 East Green Street Pasadena, CA 91106	
Mr. Charles Miller, Code 05R13 Crystal Plaza #6 Naval Sea Systems Command Washinton, DC 20362	

Heat Exchanger Branch, Code 5223
National Center #3
Naval Sea Systems Command
Washington, DC 20362

Mr. Ed Ruggiero, NAVSEA 08
National Center #2
Washington, DC 20362

Dr. Earl Quandt Jr., Code 272
David Taylor Ship R&D Center
Annapolis, MD 21402

Mr. Wayne Adamson, Code 2722
David Taylor Ship R&D Center
Annapolis, MD 21402

Dr. Win Aung
Heat Transfer Program
National Science Foundation
Washington, DC 20550

Mr. Michael Perlsweig
Department of Energy
Mail Station E-178
Washington, DC 20545

Dr. W.H. Theilbahr
Chief, Energy Conservation Branch
Dept. of Energy, Idaho Operations Office
550 Second Street
Idaho Falls, Idaho 83401

Professor Ephriam M. Sparrow
Department of Mechanical Engineering
University of Minnesota
Minneapolis, Minnesota 55455

Professor J.A.C. Humphrey
Department of Mechanical Engineering
University of California, Berkeley
Berkeley, California 94720

Professor Brian Launder
Thermodynamics and Fluid Mechanics Division
University of Manchester
Institute of Science & Technology
P088 Sackville Street
Manchester M601QD England

Professor Shi-Chune Yao
Department of Mechanical Engineering
Carnegie-Mellon University
Pittsburgh, PA 15213

Professor Charles B. Watkins
Chairman, Mechanical Engineering Department
Howard University
Washington, DC 20059

Professor Adrian Bejan
Department of Mechanical Engineering
University of Colorado
Boulder, Colorado 80309

Professor Donald M. McEligot
Department of Aerospace and Mechanical Engineering
Engineering Experiment Station
University of Arizona 85721

Professor Paul A. Libby
Department of Applied Mechanics and Engineering Sciences
University of California San Diego
Post Office Box 109
La Jolla, CA 92037

Professor C. Forbes Dewey Jr.
Fluid Mechanics Laboratory
Massachusetts Institute of Technology
Cambridge, Massachusetts 02139

Professor William G. Characklis
Dept. of Civil Engineering and Engineering Mechanics
Montana State University
Bozeman, Montana 59717

Professor Ralph Webb
Department of Mechanical Engineering
Pennsylvania State University
208 Mechanical Engineering Bldg.
University Park, PA 16802

Professor Warren Rohsenow
Mechanical Engineering Department
Massachusetts Institute of Technology
77 Massachusetts Avenue
Cambridge, Massachusetts 02139

Professor A. Louis London
Mechanical Engineering Department
Bldg. 500, Room 501B
Stanford University
Stanford, CA 94305

Professor James G. Knudsen
Associate Dean, School of Engineering
Oregon State University
219 Covell Hall
Corvallis, Oregon 97331

Professor Arthur E. Bergles
Mechanical Engineering Department
Iowa State University
Ames, Iowa 50011

Professor Kenneth J. Bell
School of Chemical Engineering
Oklahoma State University
Stillwater, Oklahoma 74074

Dr. James Lorenz
Component Technology Division
Argonne National Laboratory
9700 South Cass Avenue
Argonne, Illinois 60439

Dr. David M. Eissenberg
Oak Ridge National Laboratory
P.O. Box Y, Bldg. 9204-1, MS-0
Oak Ridge, Tennessee 37830

Dr. Jerry Taborak
Technical Director
Heat Transfer Research Institute
1000 South Fremont Avenue
Alhambra, CA 91802

Dr. Simion Kuo
Chief, Energy Systems
Energy Research Laboratory
United Technology Research Center
East Hartford, Connecticut 06108

Mr. Jack Yampolsky
General Atomic Company
P.O. Box 81608
San Diego, CA 92138

Mr. Ted Carnavos
Noranda Metal Industries, Inc.
Prospect Drive
Newtown, Connecticut 06470

Dr. Ramesh K. Shah
Harrison Radiator Division
General Motors Corporation
Lockport, New York 14094

Dr. Ravi K. Sakhuja
Manager, Advanced Programs
Thermo Electron Corporation
101 First Avenue
Waltham, Massachusetts 02154

Mr. Robert W. Perkins
Turbotec Products, Inc.
533 Downey Drive
New Britain, Connecticut 06051

Dr. Keith E. Starner
York Division, Borg-Warner Corp.
P.O. Box 1592
York, PA 17405

Mr. Peter Wishart
C-E Power Systems
Combustion Engineering, Inc.
Windsor, Connecticut 06095

Mr. Henry W. Braum
Manager, Condenser Engineering Department
Delaval
Front Street
Florence, New Jersey 08518

Dr. Thomas Rabas
Steam Turbine-Generator Technical Operations Division
Westinghouse Electric Corporation
Lester Branch
P.O. Box 9175 N2
Philadelphia, PA 19113


DAT
FILM